Best Available Copy E 2 01 744

AD-A275 567

PL-TR-93-2186

SOCRATES SIMULATION OF THE EMISSION AT WAVELENGTH 6300 Å GENERATED BY THE INTERACTION BETWEEN THE ATMOSPHERE AND THE SPACE SHUTTLE EXHAUST

A. Setayesh
M. F. Tautz

Radex, Inc.
Three Preston Court
Bedford, MA 01730

"Original contains color plates: All DTIC reproductions will be in black and white"

DTIC
ELECTE
JAN 3 1 1994
S B D

August 31, 1993

Scientific Report No. 2

Approved for public release; distribution unlimited

94-02751

PHILLIPS LABORATORY
Directorate of Geophysics
AIR FORCE MATERIEL COMMAND
HANSCOM AIR FORCE BASE, MA 01731-3010

94 1 27 005 Best Available Copy

"This technical report has been reviewed and is approved for publication"

Edward C Robinson

EDWARD C. ROBINSON
Contract Manager
Data Analysis Division

Robert E. McInerney

ROBERT E. McINERNEY, Director
Data Analysis Division

This report has been reviewed by the ESD Public Affairs Office (PA) and is releasable to the National Technical Information Service (NTIS).

Qualified requestors may obtain additional copies from the Defense Technical Information Center. All others should apply to the National Technical Information Service.

If your address has changed, or if you wish to be removed from the mailing list, or if the addressee is no longer employed by your organization, please notify PL/TSI, 29 Randolph Road, Hanscom AFB, MA 01731-3010. This will assist us in maintaining a current mailing list.

Do not return copies of this report unless contractual obligations or notices on a specific document requires that it be returned.

DISCLAIMER NOTICE

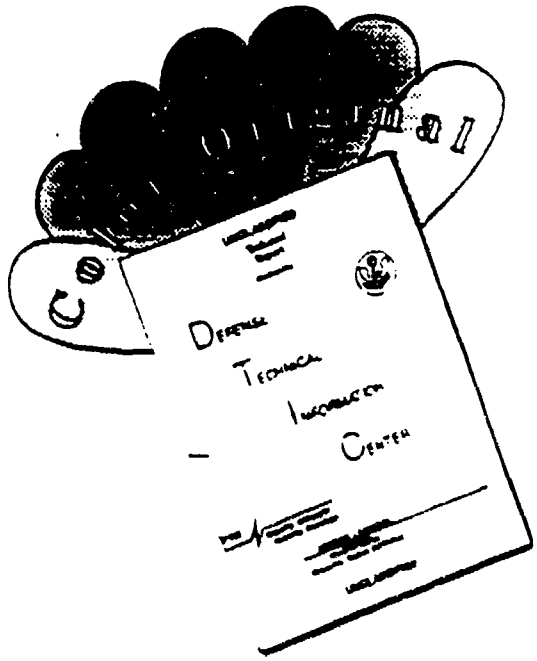

THIS DOCUMENT IS BEST QUALITY AVAILABLE. THE COPY FURNISHED TO DTIC CONTAINED A SIGNIFICANT NUMBER OF COLOR PAGES WHICH DO NOT REPRODUCE LEGIBLY ON BLACK AND WHITE MICROFICHE.

REPORT DOCUMENTATION PAGE

Form Approved
OMB No. 0704-0188

Public reporting burden for this collection of information is estimated to average 1 hour per response, including the time for reviewing instructions, searching existing data sources, gathering and maintaining the data needed, and completing and reviewing the collection of information. Send comments regarding this burden estimate or any other aspect of this collection of information, including suggestions for reducing this burden, to Washington Headquarters Services, Directorate for Information Operations and Reports, 1215 Jefferson Davis Highway, Suite 1204, Arlington, VA 22202-4302, and to the Office of Management and Budget, Paperwork Reduction Project (0704-0188), Washington, DC 20503.

1. AGENCY USE ONLY (Leave blank)	2. REPORT DATE	3. REPORT TYPE AND DATES COVERED
	31 August 1993	Scientific Report No. 2

4. TITLE AND SUBTITLE

SOCRATES Simulation of the Emission at Wavelength 6300 Å Generated by the Interaction Between the Atmosphere and the Space Shuttle Exhaust

5. FUNDING NUMBERS

PE 62101F
PR 7659 TA GY WU AA

Contract F19628-93-C-0023

6. AUTHOR(S)

A. Setayesh
M. F. Tautz

7. PERFORMING ORGANIZATION NAME(S) AND ADDRESS(ES)

RADEX, Inc.
Three Preston Court
Bedford, MA 01730

8. PERFORMING ORGANIZATION REPORT NUMBER

RXR-93082

9. SPONSORING / MONITORING AGENCY NAME(S) AND ADDRESS(ES)

Phillips Laboratory
29 Randolph Road
Hanscom AFB, MA 01731-3010

Contract Manager: Edward C. Robinson/GPD

10. SPONSORING / MONITORING AGENCY REPORT NUMBER

PL-TR-93-2186

11. SUPPLEMENTARY NOTES

12a. DISTRIBUTION / AVAILABILITY STATEMENT

Approved for Public Release
Distribution Unlimited

12b. DISTRIBUTION CODE

13. ABSTRACT (Maximum 200 words)

The SOCRATES contamination-interaction code has been used to simulate the reactions between the space shuttle exhaust and the atmosphere at an altitude of 320 km. The investigation carries out the simulations for regions extending to 15 km from spacecraft. These simulations calculate the radiation from $O(^1D) \rightarrow O(^3P)$ photons as function of time for orientations of engine firing into the ram, perpendicular, and into the wake of the shuttle motion. The IRMA plotting program has been used to depict in color the time development of the shuttle plume.

14. SUBJECT TERMS

SOCRATES computer code, Monte Carlo method, Gas plume, Photon emission, (O^1D) excitation

15. NUMBER OF PAGES

16. PRICE CODE

17. SECURITY CLASSIFICATION OF REPORT	18. SECURITY CLASSIFICATION OF THIS PAGE	19. SECURITY CLASSIFICATION OF ABSTRACT	20. LIMITATION OF ABSTRACT
Unclassified	Unclassified	Unclassified	Unlimited

TABLE OF CONTENTS

Section		Page
1.	INTRODUCTION	1
2.	SOCRATES METHOD OF SIMULATION	2
3.	DESCRIPTION OF THE EXPERIMENT AND CONFIGURATION MODEL	4
4.	DISCUSSION OF RESULTS	8
5.	SUMMARY AND CONCLUSION	33
	REFERENCES	34

DTIC QUALITY INSPECTED 2

Accession For
NTIS GRA&I ☑
DTIC TAB ☐
Unannounced ☐
Justification
By
Distribution/
Availability Codes
Dist | Avail and/or Special
A-1

LIST OF FIGURES

Figure — Page

1. Contour plots showing the calculated 6300 Å plume radiance for a ram burn at several time steps. The shuttle is located at the origin of coordinates, and the wind is flowing to the right 9

2. Contour plots showing the calculated 6300 Å plume radiance for a perpendicular burn at several time steps. The shuttle is located at the origin of coordinates, and the wind is flowing to the right 10

3. Contour plots showing the calculated 6300 Å plume radiance for a wake burn at several time steps. The shuttle is located at the origin of coordinates, and the wind is flowing to the right 11

4. The temporal dependence of $O(^1D)$ emission for the three orientations. This emission is integrated spatially over a region of about 20 by 20 km around the shuttle 13

5. This figure is same as Figure 4, except that it is calculated from the number density and lifetime of $O(^1D)$ 14

6. The temporal dependence of $O(^1D)$ reaction rate for the three orientations. This emission is integrated spatially over a region of about 20 by 20 km around the shuttle 15

7. Photon emission at 6300 Å for ram burn before shutdown 16

8. Photon emission at 6300 Å for ram burn after shutdown 17

9. Photon emission at 6300 Å for perpendicular burn before shutdown . 18

10. Photon emission at 6300 Å for perpendicular burn after shutdown . . 19

11. Photon emission at 6300 Å for wake burn before shutdown 20

List of Figures (cont'd)

Figure		Page
12.	Photon emission at 6300 Å for wake burn after shutdown	21
13.	O and $O(^1D)$ densities on an arbitrary central z plane slice	23
14.	Charged O and charged H_2O densities on an arbitrary central z plane slice	24
15.	N_2 and H_2O densities on an arbitrary central z plane slice, plotted based on the maximum and upper values of the densities	25
16.	N_2 and H_2O densities on an arbitrary central z plane slice, plotted based on lower values of the densities	26
17.	CO and H_2 densities on an arbitrary central z plane slice	27
18.	CO_2 and OH densities on an arbitrary central z plane slice	28
19.	Reaction rates on an arbitrary central z plane slice, for reaction given above	29
20.	Reactions rates on an arbitrary central z plane slice, for reaction given above	30
21.	Reactions rates on an arbitrary central z plane slice, for reaction given above	31
22.	Reactions rates on an arbitrary central z plane slice, for reaction given above	32

LIST OF TABLES

Table		Page
1.	Concentrations of Species in the SOCRATES Simulation	5
2.	Molecular Parameters Used in the Calculations	6
3.	Rate Coefficient Used in SOCRATES, $k = A\ T^n \exp(-E_a/kT)$	7
4.	Parameters Used in the Simulations	8

ACKNOWLEDGEMENTS

The authors wish to thank Edmond Murad, Phillips Laboratory, Spacecraft Interactions Branch, for initiation of this work, and his valuable comments and advice throughout the course of this investigation. The acknowledgement is also extended to Jim Elgin, Spectral Sciences, Inc. for providing the SOCRATES, MAP, and CONTOUR codes to accomplish this investigation and to David Cooke, Phillips Laboratory, Spacecraft Interactions Branch, for helpful advice during the course of the work and valuable comments on color graphics presentation of the figures.

1. INTRODUCTION

The interactions between the exhaust from the shuttle Primary Reaction Control System (PRCS) engine firings and the ambient atmosphere were investigated using the SOCRATES code. The calculations are compared to ground-based data observed from the Air Force Maui Optical Station (AMOS) [*Broadfoot, et al.*, 1992]. Data were obtained for the shuttle at an altitude of 320 km, for three angles of attack (180, 90, and 0 degrees) corresponding to firings into the ram, perpendicular, and into the wake of the shuttle direction of motion, respectively. The data analyses of this experiment and some modeling efforts have been investigated by *Broadfoot, et al.* [1992] and *Elgin, et al.* [1991]. The modeling efforts here are focused mainly on simulating the general character of the plumes in the three orientations, and trying to understand the characteristics of the emission at 6300 Å. This feature is attributed to the atomic oxygen red line emission from transition between the $O(^1D)$ excited state and the $O(^3P)$ ground state. Two processes were considered for formation of $O(^1D)$: excitation of atmospheric $O(^3P)$ by collision with the exhaust of the shuttle engines, and charge exchange between O^+ and exhaust H_2O.

The SOCRATES calculations have been done for each of the three angles of attack. The following sections summarize this simulation work. Section 2 outlines the SOCRATES code algorithms. In Section 3, we describe the AMOS measurements and the SOCRATES model representation of the experiment. Section 4 presents the simulation results in the form of temporal and spatial distributions of the emissions. Section 5 gives a summary and conclusion of the investigation.

2. SOCRATES METHOD OF SIMULATION

The SOCRATES code is based on the direct simulation Monte Carlo technique that provides a powerful tool for the simulation of real gas flows [*Bird*, 1981]. The SOCRATES contamination-interaction program has been developed to account for contamination on spacecraft and to study the neighboring flow field around the shuttle [*Elgin and Sundberg*, 1988]. The direct simulation Monte Carlo method has been revised and extended significantly to account for energy dependent collision cross sections and a statistical model for internal energy effects [*Borgnakke and Larsen*, 1975] and [*Elgin and Sundberg*, 1988]. The method is briefly described here. The solution region is a network of cells of different sizes. Initially, a discrete number of molecules are stored in the computer, based on their velocity components, position coordinates, and other necessary information. The molecular motion and intermolecular collisions in the simulated region advance and are modified with time, in a two-stage process. In the first stage, the molecules are propagated along their trajectories according to their velocity components and the time increment. At this stage, some of the molecules may leave the solution domain and some will be introduced according to the boundary conditions of the problem. In the second stage, a typical set of collisions will be simulated among the molecules in each cell with appropriate time increment. The repetition of these two stages over the small time interval will uncouple the molecular motion and intermolecular collisions. In a SOCRATES simulation, the solution is periodically sampled by accumulating statistical sums of number densities, velocities and other basic properties. The solution is run repeatedly until statistical deviations are reduced to a desired limit, and the physically meaningful output quantities are computed from the statistical sums. The number of molecules represented are typically many thousands at a time, which is much smaller than the number of molecules occurring in real flows. Therefore, the construction of a dynamically similar flow to be simulated in the computer is an essential feature of the method [*Elgin and Bernstein* ,1992].

In the code, the collision cross section is defined by the variable hard sphere model (VHS) which depends on the relative velocity v_r between two molecules. The collision cross section can be stated as

$$\sigma = \sigma_{ref} \left(\frac{v_r}{v_{ref}}\right)^{-2\omega} \quad (1)$$

where σ_{ref} and v_{ref} are the reference collision cross section and velocity, respectively [*Elgin, et al.*,1990]. ω is a constant parameter that has a value of 0.25 for this investigation.

Reactive collisions between molecules and/or atoms can be simulated directly by SOCRATES. The Monte Carlo program simulates the reaction with a probability that is related to the ratio of the reactive to collision cross section at the relative velocity for the collision [*Elgin and Sundberg*, 1992].

The present work employs the option of using the Arrhenius rate constant in the code to calculate the reactive collision cross section. The rate constant has the form of

$$k_r = A\ T^n\ e^{-\frac{E_a}{R_0 T}} \quad (2)$$

where A and n are constant parameters, R_0 and T are gas constant and temperature, respectively, and E_a is the activation energy. The reactive cross section, σ^*, corresponding to Equation (2), depends on the relative collision energy and is given by [*Bird*, 1981]

$$v_r \sigma^* = \frac{\sqrt{\pi}\ (1 + \delta_{ij})\ A}{2R_o^n\ \Gamma\ (n + \frac{3}{2})} \sqrt{1 - \frac{E_a}{E_c}} (E_c - E_a)^n \quad (3)$$

Here, E_c is the collision energy, δ_{ij} is unity for like reactants and zero for unlike reactants, and Γ is the gamma function. In the case of collision between two

molecules, the reactive cross section is calculated, and the reaction is counted with a weighting factor W_r. The weighting factor is given by

$$W_r = W_c \frac{\sigma^*}{\sigma} \tag{4}$$

where σ^*, σ, and W_c are the reactive cross section, collision cross section, and collision weighting factor, respectively. Further discussion of the reactive collisions can be found in the report by *Elgin and Sundberg* [1992].

3. DESCRIPTION OF THE EXPERIMENT AND CONFIGURATION MODEL

The experiment was based on firing the Primary Reaction Control System engines of the space shuttle. The PRCS liquid-fuel engines were fired in the ram, wake, and perpendicular directions (angles of attack of 180°, 0°, and 90° respectively). The experiment was performed on October 7, 1990 at 1326 UT, while the Shuttle overflew the Air Force Maui Optical Station. The shuttle was in the 300-km altitude range. The imagery data from PRCS engine firings were obtained using an Intensified Charged-Coupled Device (ICCD) spectrograph at the focus of a 200-mm aperture, f/5 telescope mounted on and coaligned with a 1.6 m telescope. The details and discussion of data acquisition and analysis of the experiment can be found in reference [*Broadfoot, et al.*, 1992].

The main purpose of our investigation is to simulate this experiment using the SOCRATES code. Therefore, considerable care has been given to use a realistic set of species, chemical and photochemical reactions, and parameters for the PRCS engine and ambient atmosphere. The solution domain for the simulations is taken to be a space of dimensions 21 by 20 by 20 km consisting of 3332 unevenly spaced cells. In each cell there are 3 to 20 molecules (depending on density of species and cell location) for each species. This setup has generally been retained for all three firings in the ram, perpendicular, and wake directions. All of the species and their reactions and most of the important parameters which have been used for the simulation are given in Tables 1-4.

The exhaust and atmospheric mole fractions of the species used in the calculations are given in the Table 1. Since the other species present in the atmospheric composition have no significant effect on the problem, they have not been considered in the calculations.

TABLE 1. Concentrations of Species in the SOCRATES Simulation

Species	Atmospheric Mole Fraction	Exhaust Mole Fraction
O	0.9076	0.0
N_2	0.0919	0.309
O^+	0.0005	0.0
H_2O	0.0	0.332
H_2	0.0	0.187
CO	0.0	0.136
CO_2	0.0	0.036

Table 2 shows a list of the species used in the simulations. These species represent engine exhaust, as well as atmospheric ambient compositions and reactions products. The table also lists the reference collision cross-section σ_{ref}, between two members of this species, corresponding reference relative collision velocity v_{ref}, number of internal degrees of freedom v_i, and heat of formation for the species.

TABLE 2. Molecular Parameters Used in the Calculations

Species	σ_{ref} (cm^2)	v_{ref} (cm/s)	Heat of Formation (kcal/mole)	v_i
O	1.750×10^{-15}	2.490×10^5	59.60	0.00
N_2	3.540×10^{-15}	2.130×10^5	0.00	2.00
O^+	1.395×10^{-14}	2.490×10^5	372.40	0.00
H_2O	3.270×10^{-15}	2.290×10^5	-57.80	3.76
H_2	1.860×10^{-15}	7.740×10^5	0.00	3.29
CO	3.460×10^{-15}	2.090×10^5	-26.42	2.00
CO_2	4.330×10^{-15}	1.710×10^5	-94.10	3.58
$O(^1D)$	1.750×10^{-15}	2.490×10^5	104.90	0.00
OH	1.770×10^{-15}	8.000×10^5	9.40	2.00
H_2O^+	3.270×10^{-15}	2.290×10^5	232.70	3.76

Table 3 lists the chemical reactions used in the simulations. There are generally two types of mechanisms for generating $O(^1D)$ given in the table:

the charge exchange reaction

$$H_2O + O^+ \rightarrow H_2O^+ + O(^1D)$$

and

$$O(^3P) + X \rightarrow O(^1D) + X$$

where X is any exhaust species with sufficient kinetic energy to excite the $O(^1D)$. For example, in Table 3, X represents N_2, $O(^3P)$, and H_2O. The $O(^1D)$ can undergo four quenching reactions as shown in Table 3, which do not produce photons. The photochemical decay,

$$O(^1D) \rightarrow O(^3P) + h\nu \ (\lambda = 6300 \text{ Å})$$

is proposed to generate the photon emission at 6300 Å. The table also shows the values used for the Arrhenius rate coefficients for the different reactions. The discussion of the constants in Table 3 can be found in the reference [*Broadfoot, et al.*, 1992].

TABLE 3. Rate Coefficient Used in SOCRATES, $k = A\ T^n \exp(-E_a/kT)$

Reaction	A	n	E_a (kcal/ mole)	Reaction ΔH (kcal/mole)
$O(^3P) + N_2 \rightarrow O(^1D) + N_2$	1.28×10^{-11}	0.0	45.3	45.3
$O(^3P) + O(^3P) \rightarrow O(^1D) + O(^3P)$	4.9×10^{-12}	0.0	45.3	45.3
$O(^3P) + H_2O \rightarrow O(^1D) + H_2O$	1.28×10^{-12}	0.0	45.3	45.3
$O(^1D) + N_2 \rightarrow O(^3P) + N_2$	2.3×10^{-11}	0.0	0.0	-45.3
$O(^1D) + O(^3P) \rightarrow O(^3P) + O(^3P)$	8.0×10^{-12}	0.0	0.0	-45.3
$O(^1D) + H_2O \rightarrow O(^3P) + H_2O$	2.3×10^{-11}	0.0	0.0	-45.3
$O(^1D) + H_2O \rightarrow OH + OH$	2.2×10^{-10}	0.0	0.0	-28.3
$H_2O + O^+ \rightarrow H_2O^+ + O(^1D)$	3.23×10^{-9}	-0.03	23.0	23.0
$O(^1D) \rightarrow O(^3P)$ (photochemical)	1.5×10^2 (lifetime, seconds)			

Table 4 represents the summary of information for the ambient environment and PRCS engine exhaust burns released into space. The first four parameters given in the table show the ambient conditions, and the rest are exhaust system parameters.

TABLE 4. Parameters Used in the Simulations

Altitude	320 km
Velocity of Spacecraft	7.4 km/s
Atmospheric Temperature	925° K
Atmospheric Number density	5.74×10^{8} cm^{-3}
Mass Flow	1.227×10^{3} g/s
Exit Plane Area	4.66×10^{2} cm^{2}
Ratio of Specific Heat	1.297
Exit Mach Number	4.02
Exit Nozzle Half Angle	8.0°
Exit Plane Density	8.872×10^{-6} g/cm^{3}
Exit Plane Number Density	2.618×10^{17} molecules/cm^{3}
Exit Plane Velocity	2.969×10^{5} cm/s
Exit Plane Speed of Sound	7.386×10^{4} cm/s
Exit Plane Temperature	1.032×10^{3}° K
Exit Plane Pressure	3.731×10^{4} dynes/cm^{2}
Thrust	8.584×10^{2} lb

4. DISCUSSION OF RESULTS

The results discussed here are based on a time dependent simulation using the SOCRATES code for calculating the distribution of $O(^1D) \rightarrow O(^3P)$ photons. The problem was simulated in 20 time steps, spanning 8.0 seconds beginning with the start of the engine. It was assumed that the PRCS engine was shut down at 3.0 seconds after it started. The plots presented here are a representative selection of the 20 step times. The simulations were performed in three directions of ram, perpendicular, and wake.

Figures 1-3 show the contour plots for the evolution of the 6300 Å plume in radiance (Watts/steradian/cm^2) for $O(^1D) \rightarrow O(^3P)$ transition as a function of time for ram, perpendicular, and wake burns, respectively. In these figures, the calculated results are plotted for six step times: two contour plots before shutdown of the engine, one at the time of shutdown (3.0 sec), and three contour plots after the shutdown of the engines. As can be seen from the figures (especially the ram

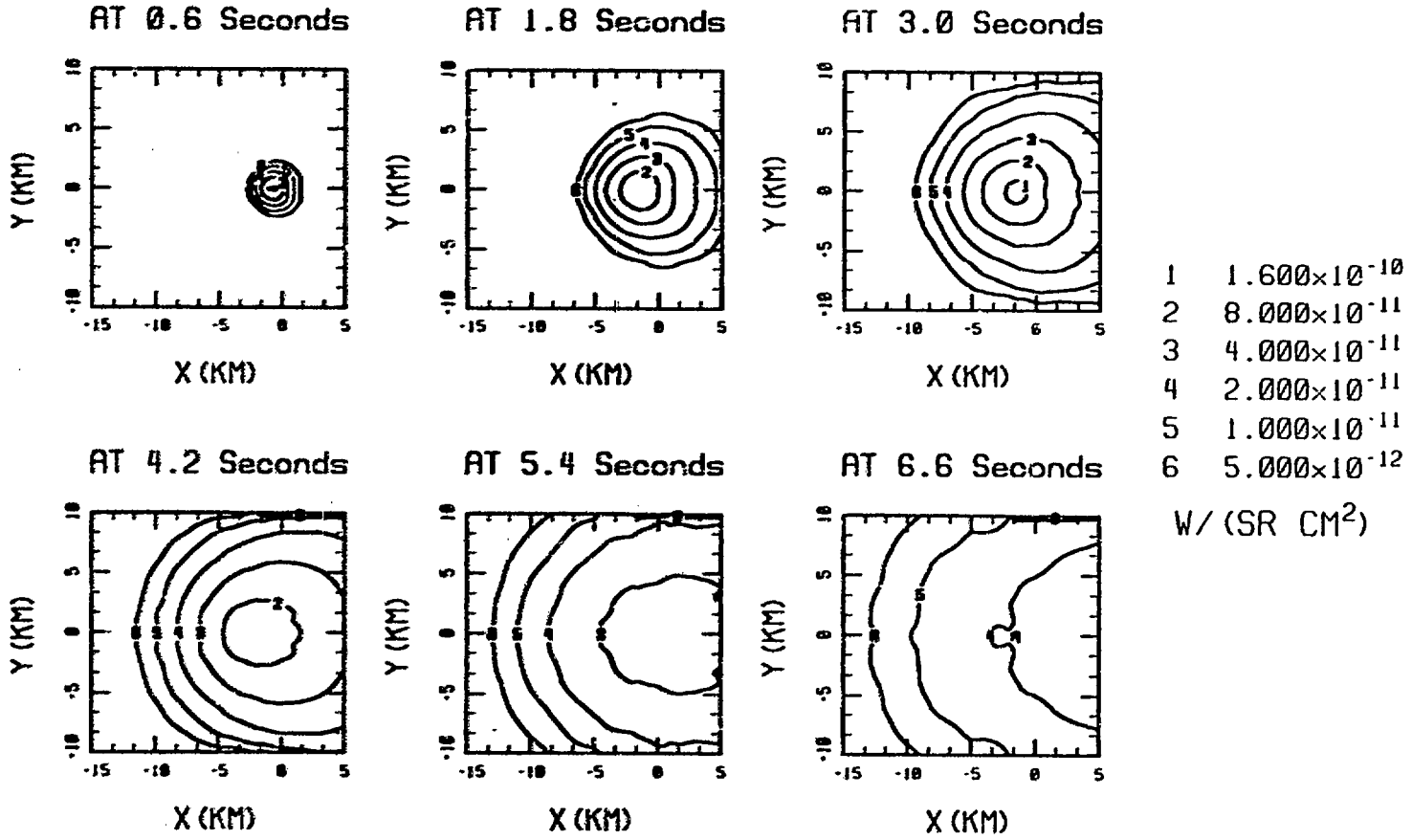

Figure 1. Contour plots showing the calculated 6300 Å plume radiance for a ram burn at several time steps. The shuttle is located at the origin of coordinates, and the wind is flowing to the right.

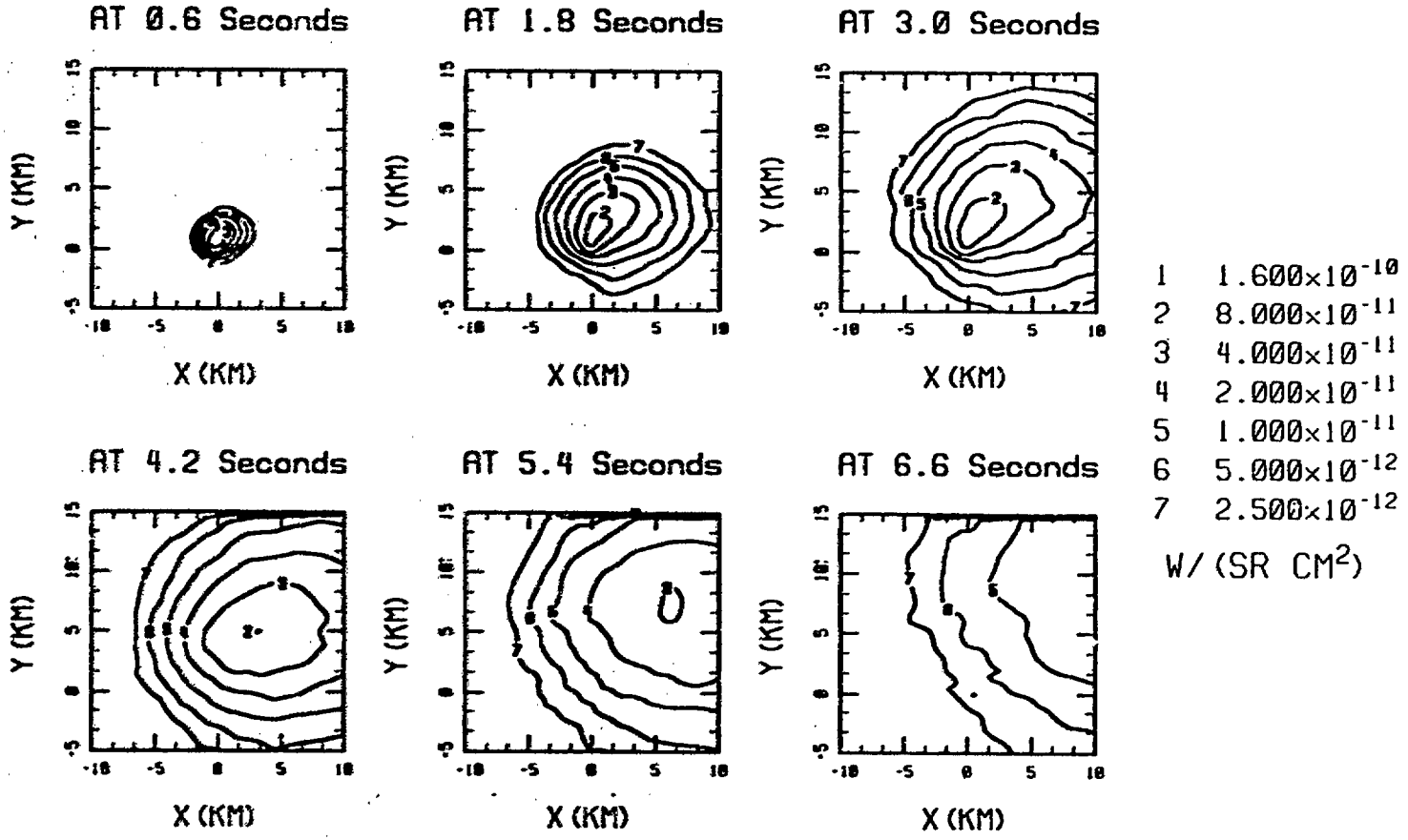

Figure 2. Contour plots showing the calculated 6300 Å plume radiance for a perpendicular burn at several time steps. The shuttle is located at the origin of coordinates, and the wind is flowing to the right.

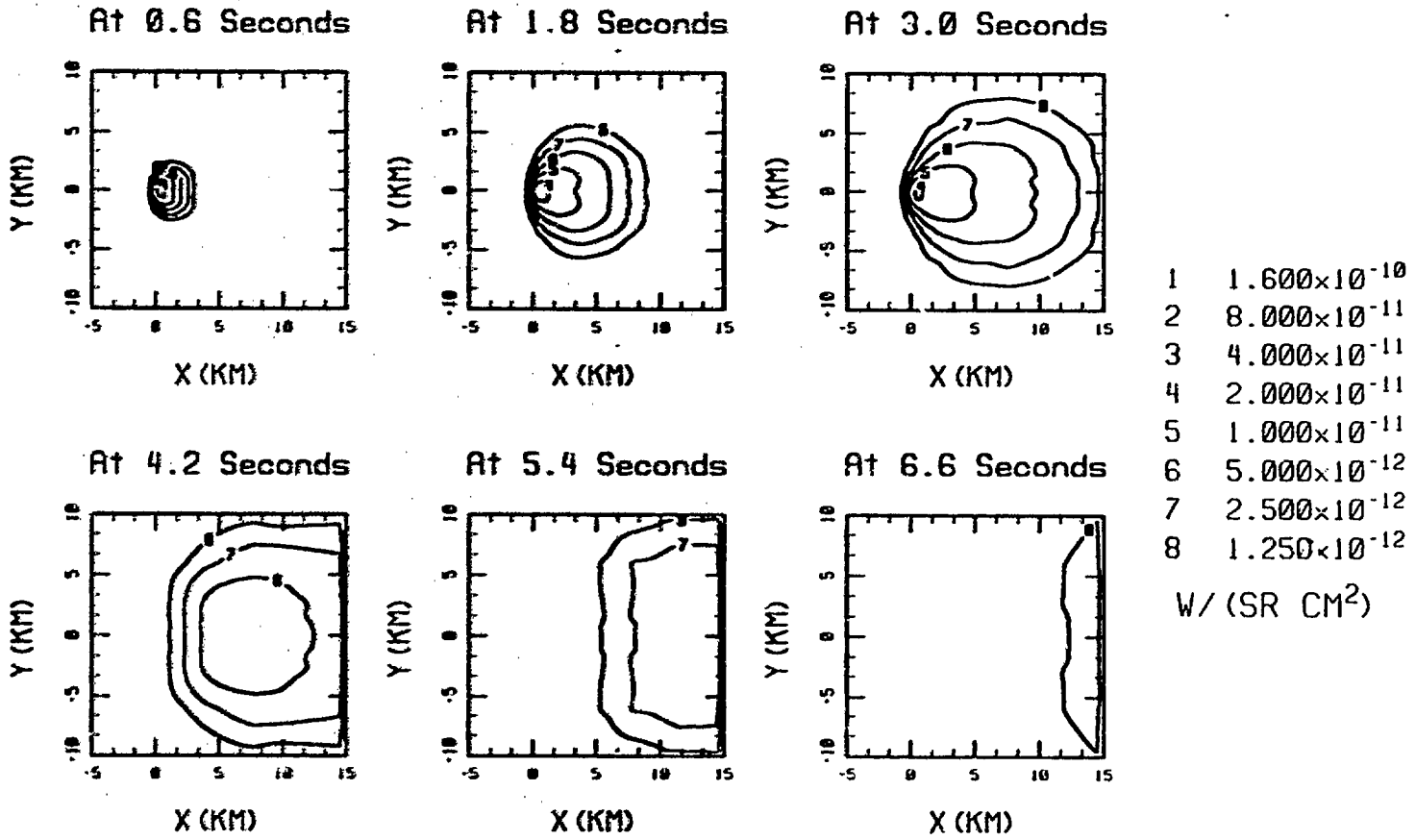

Figure 3. Contour plots showing the calculated 6300 Å plume radiance for a wake burn at several time steps. The shuttle is located at the origin of coordinates, and the wind is flowing to the right.

case, Figure 1), the relatively slow radiance decay after the engine shutdown is due to the long radiative lifetime of $O(^1D)$. The emission disappears mostly due to diffusion of $O(^1D)$.

Figures 4-5 show the radiant intensity (Watts/steradian) for 6300 Å emission as a function of time in the three directions of ram, perpendicular, and wake. Figure 4 is plotted based on the SOCRATES calculation of radiant intensity in Watts/(sr cm^2). Using an auxiliary program called MAP, this data was integrated through the line of sight to give radiance in Watts/sr. The radiant intensity in Watts/sr can also be calculated from the SOCRATES output of the $O(^1D)$ number density. Using the MAP program, the total number of excited molecules, N, in the field of view is obtained. From this, we can calculate the average decay rate as N/τ where τ is the lifetime for the excited state. The energy emitted by each photon is $\Delta e = hc/\lambda$ where h = Plank's constant, c is the speed of light, and λ is the wavelength. Hence, the total energy emitted per second is $e = N/\tau\ \Delta e$ and the energy per steradian is $E = e / (4\ \pi)$. In Watts/sr, $E = (N/\tau\ 1/\lambda\ 1.99 \times 10^{-19})$, where λ is in micron. Figure 5 is based on the density variations of $O(^1D)$ vs. time in the directions of ram, perpendicular, and wake. The calculation proceeded as described above using the density and life time of $O(^1D)$, and a converting factor to obtain the radiant intensity (Watts/steradian). Figures 4 and 5 are almost identical, as expected. Figure 6 shows the decay rate (reactions/sec) obtained from the MAP program for the reaction $O(^1D) \rightarrow O(^3P)$ photons. This plot is proportional to Figure 4, but given in different units. It should also be noted that Figures 4-6 were calculated using the field of view of 20 by 20 km.

Figures 7-12 show the same cases as for Figures 1-3, but depicted in color to better represent the morphology of the plumes. The color plots were created using the IRMA program [*Tautz*, 1993]. This code can read the SOCRATES output files to extract the reaction data, and then integrate along an arbitrary line of sight to compute the plume radiance. There are two sets of plots for each case (ram, perpendicular, and wake firing). The first set of four frames shows the development of the plume up to the engine shut off time (3 sec.) and the second set shows the dispersion of the plume after shut off. In each plot, the shuttle is located at the origin of the (x,y) coordinates indicated in the frames. The viewing window is 16 by 16 km, and the length of the x-y axis is 1 km. In the simulation, the shuttle velocity is in the negative x direction, so that in the shuttle rest frame the ambient environment flows from left to right. A common color legend, representing radiance in Watts/(sr cm^2), has been used for all the frames. It is

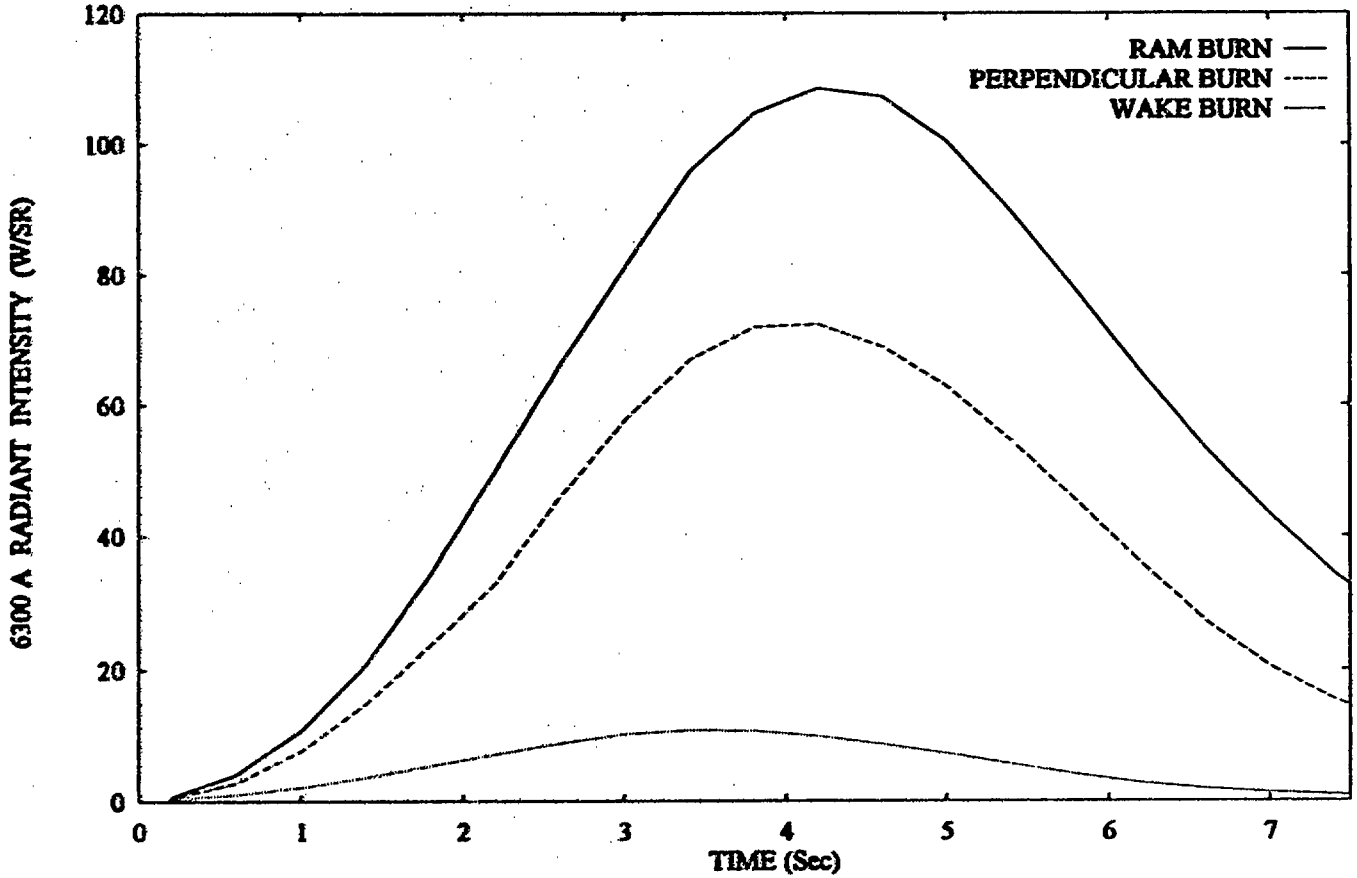

Figure 4. The temporal dependence of $O(^1D)$ emission for the three orientations. This emission is integrated spatially over a region of about 20 by 20 km around the shuttle.

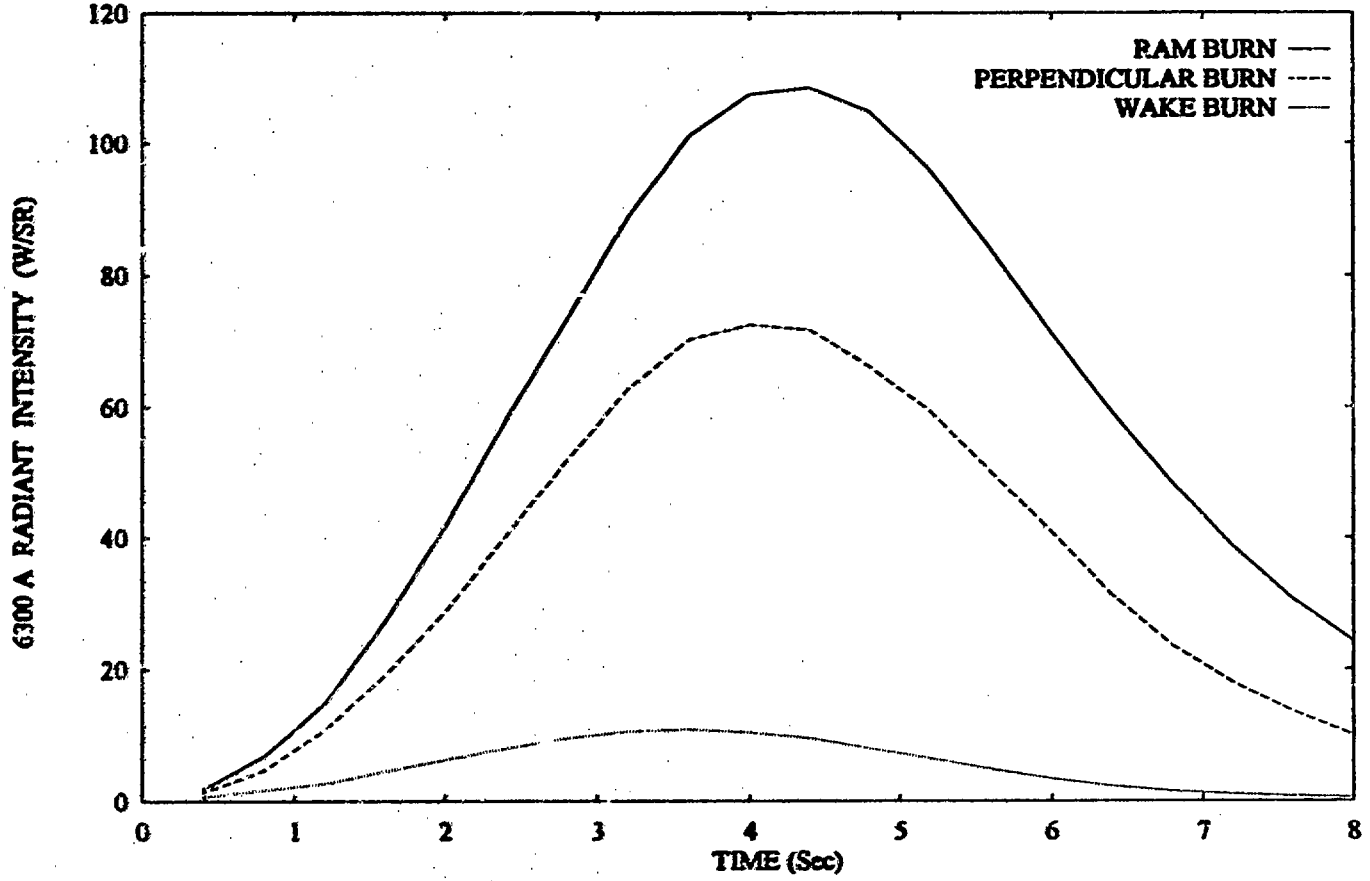

Figure 5. This figure is same as Figure 4 except that, it is calculated from the number density and lifetime of $O(^1D)$.

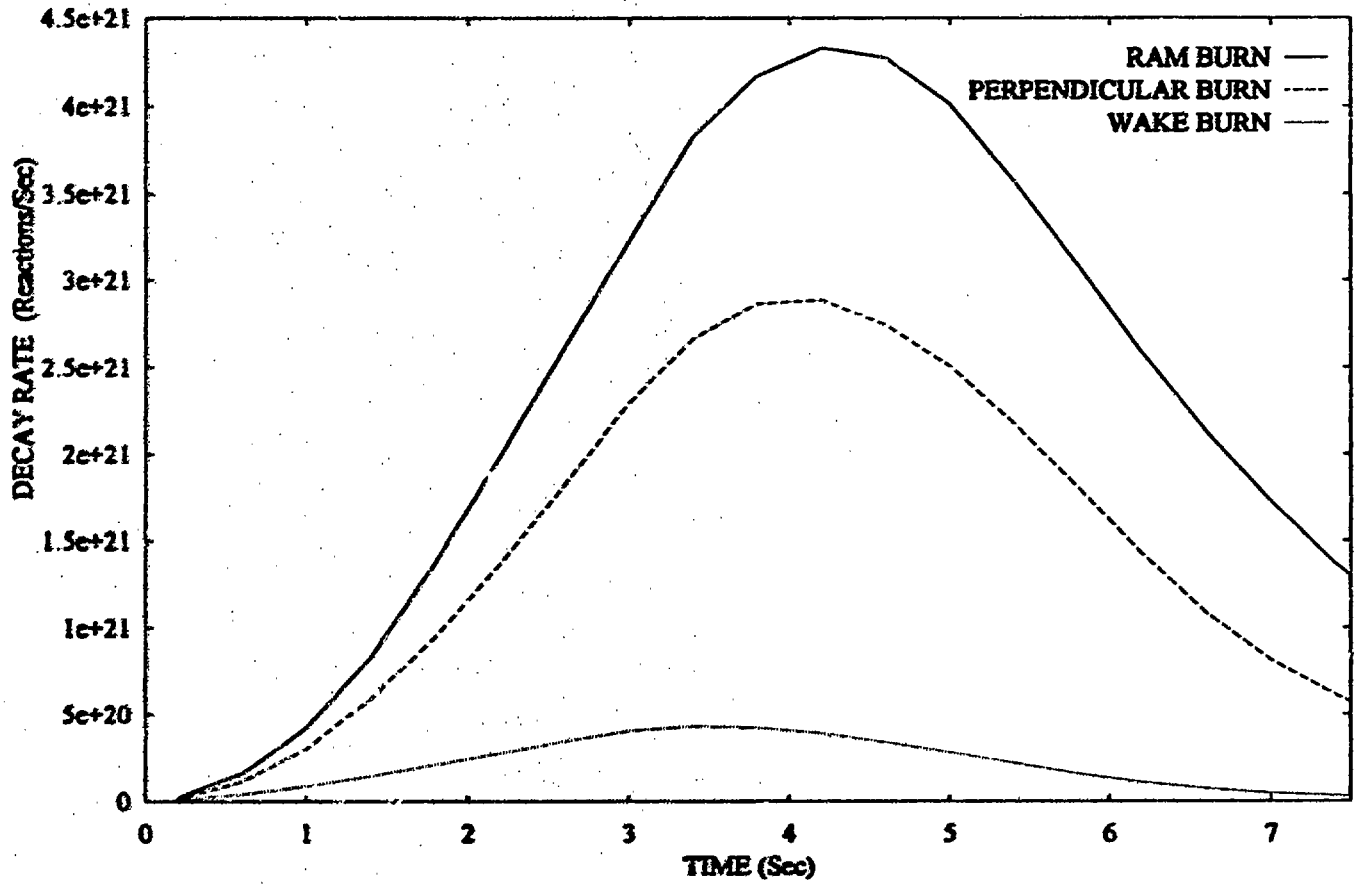

Figure 6. The temporal dependence of $O(^1D)$ reaction rate for the three orientations. This emission is integrated spatially over a region of about 20 by 20 km around the shuttle.

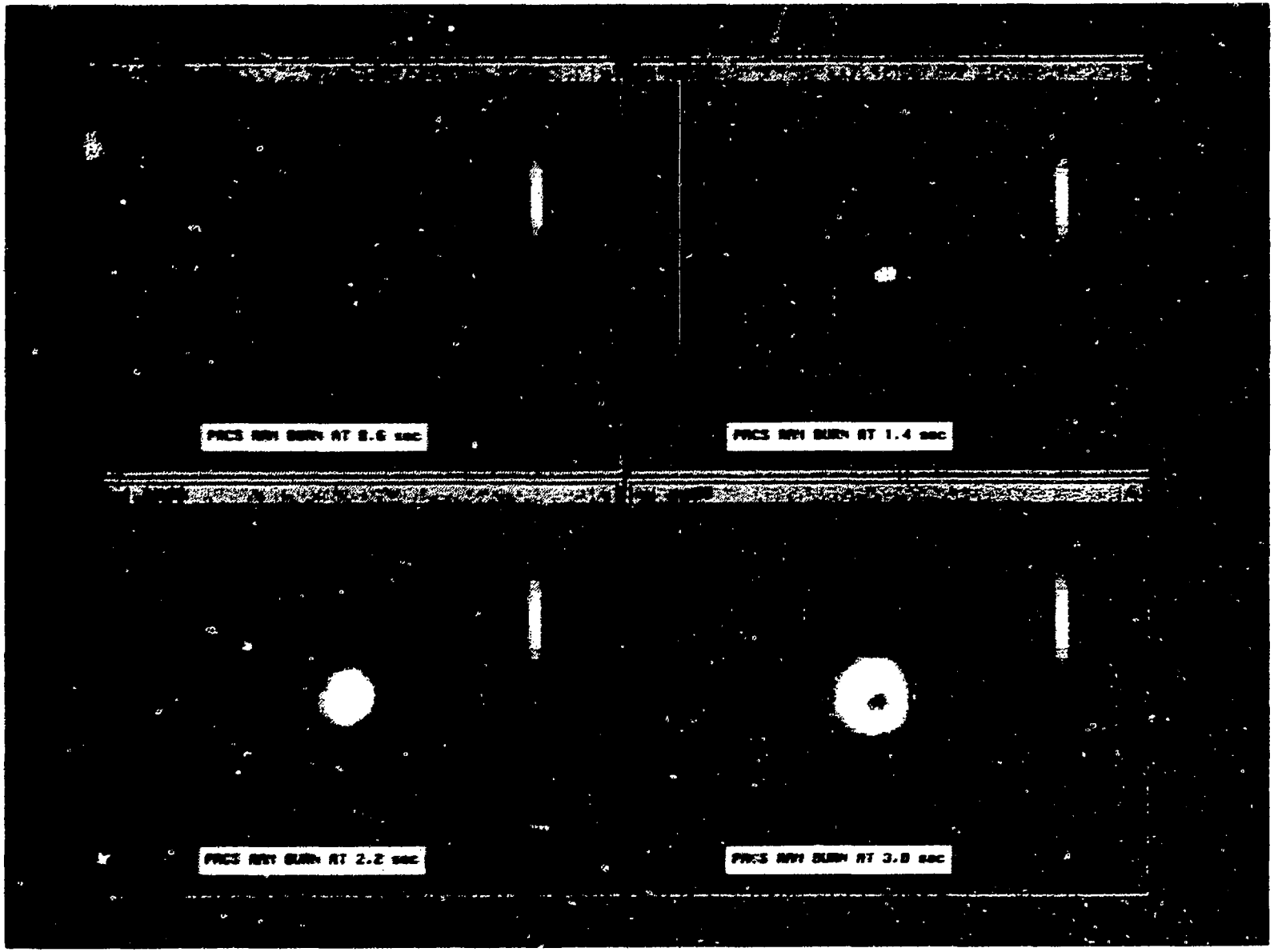

Figure 7. Photon emission at 6300 Å for ram burn before shutdown.

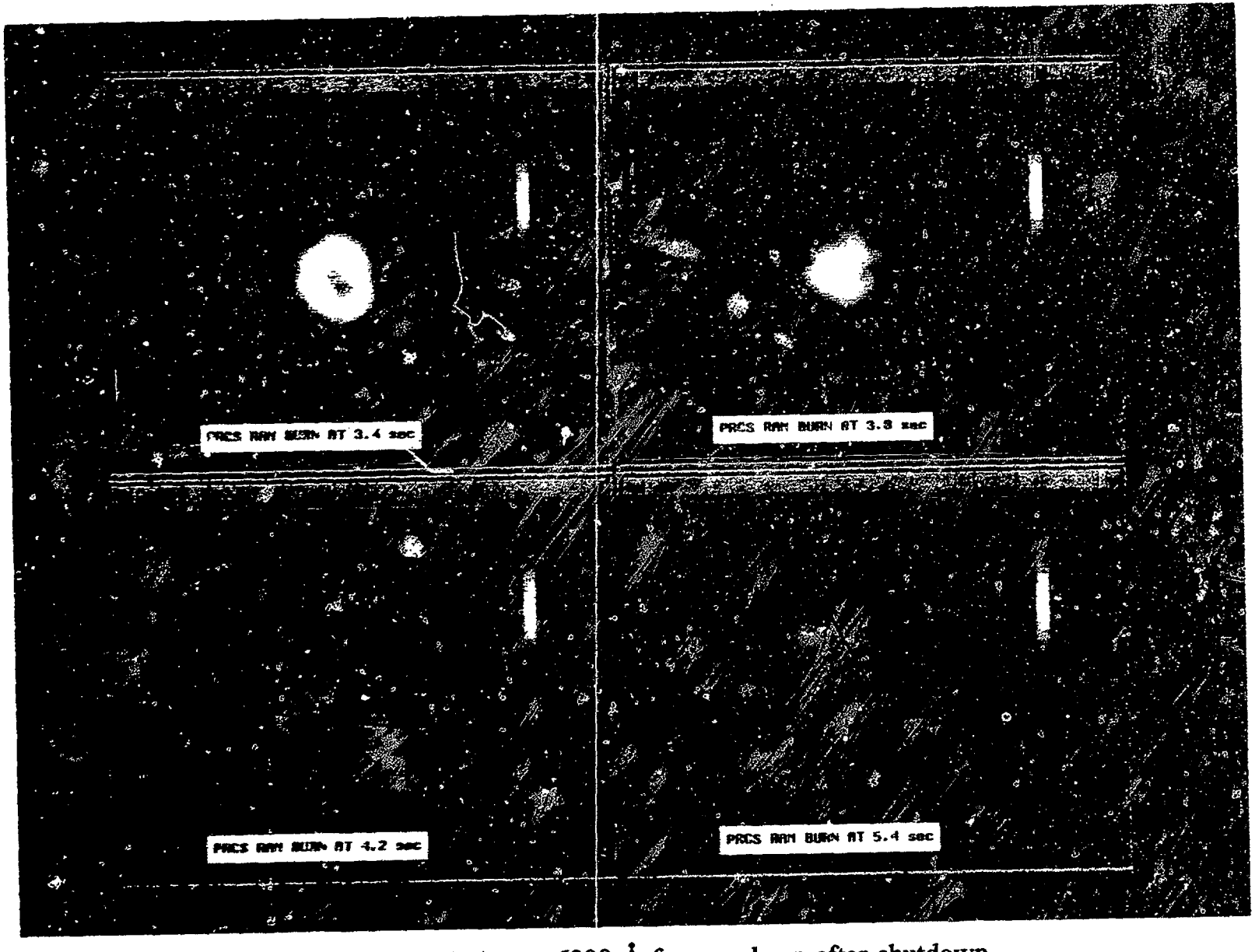

Figure 8. Photon emission at 6300 Å for ram burn after shutdown.

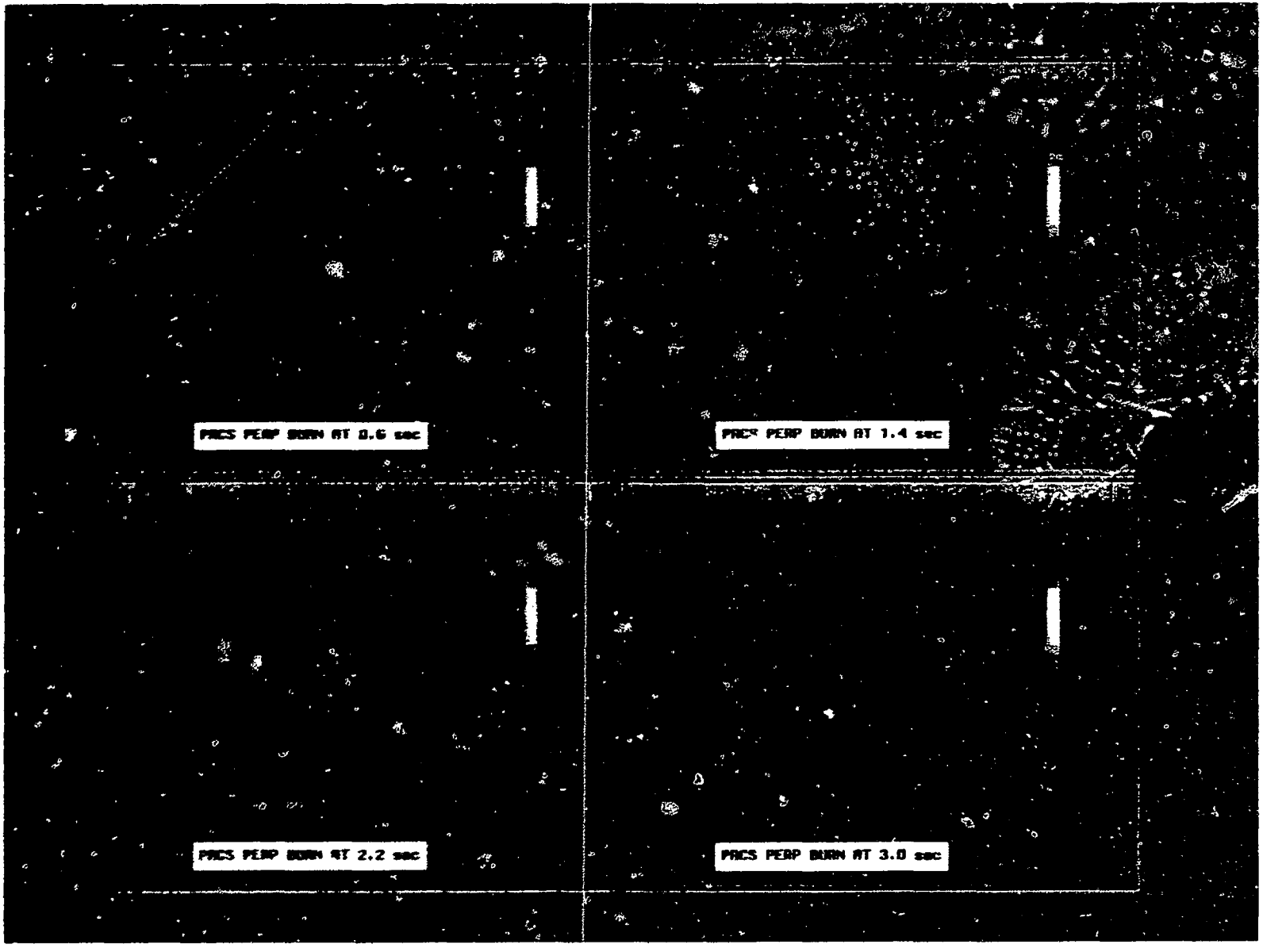

Figure 9. Photon emission at 6300 Å for perpendicular burn before shutdown.

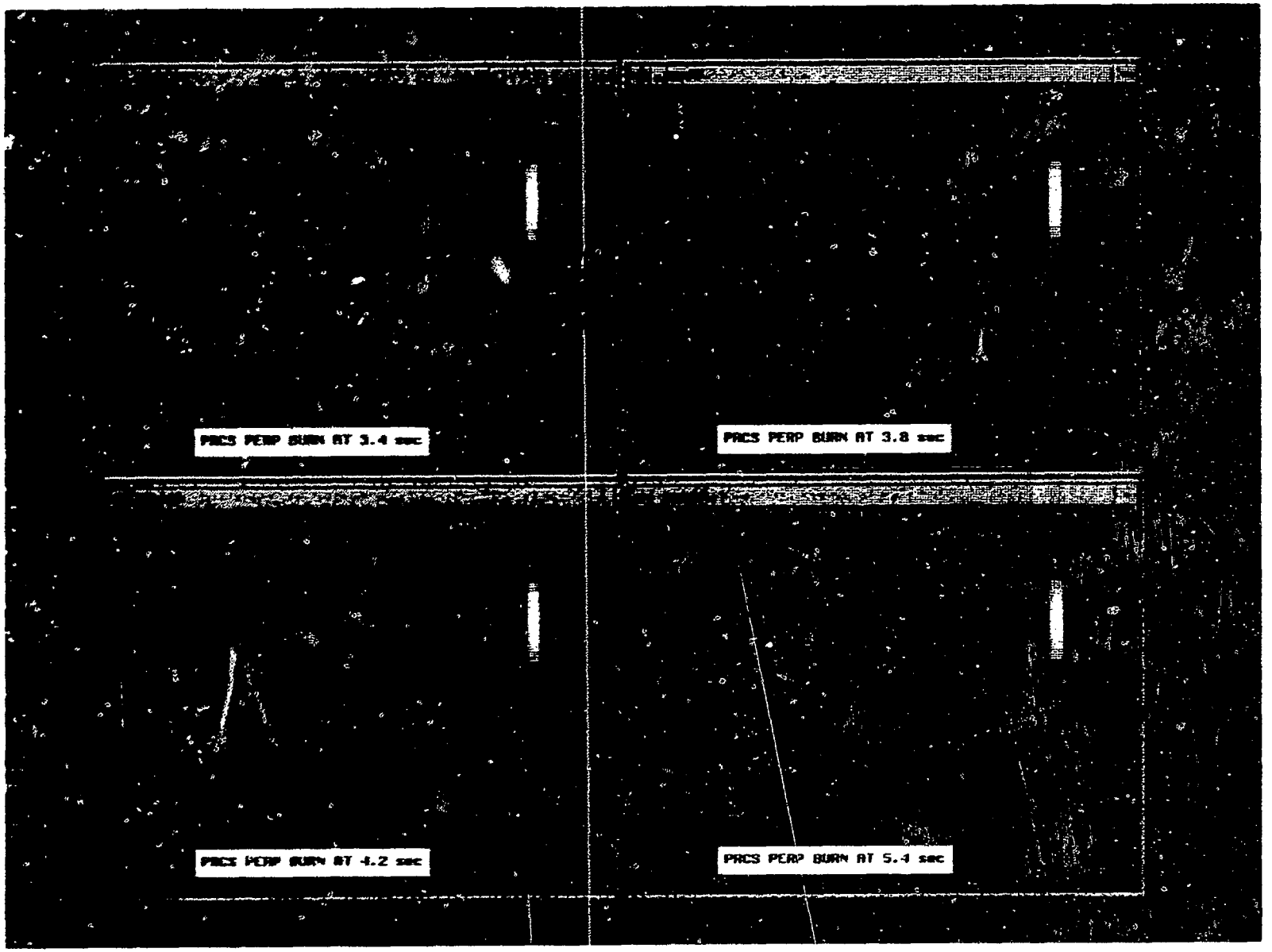

Figure 10. Photon emission at 6300 Å for perpendicular burn after shutdown.

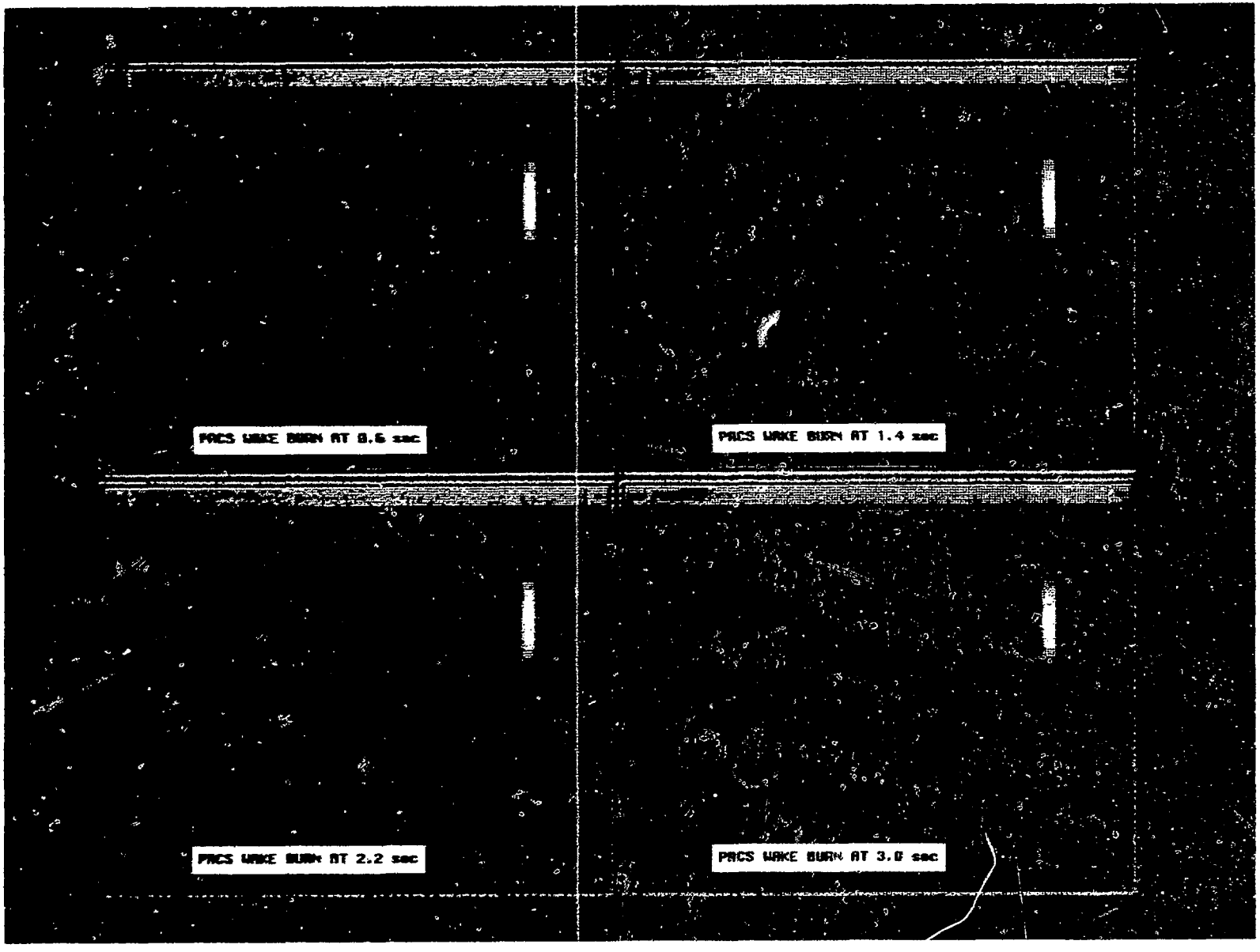

Figure 11. Photon emission at 6300 Å for wake burn before shutdown.

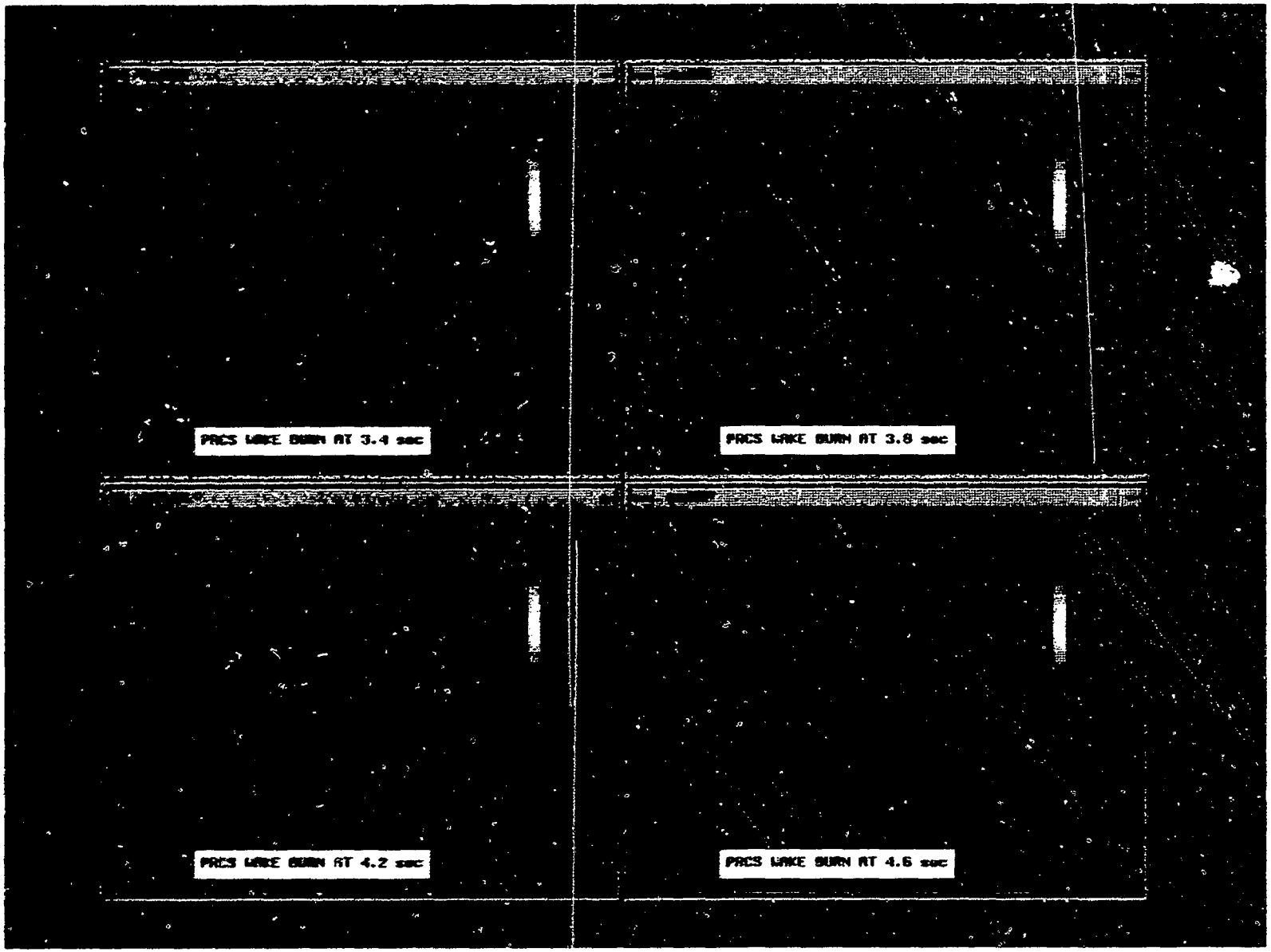

Figure 12. Photon emission at 6300 Å for wake burn after shutdown.

evident that the ram burn produces the most intense plume, followed by the perpendicular burn, and that the wake burn is barely visible on this scale.

The results that have been discussed thus far are concerned with the $O(^1D)$ photon emission. However, for better presentation of the problem, it is important to study the behavior of the other species and their reactions in the simulation. Therefore, a brief discussion of the simulation for the rest of the species which are illustrated in Tables 2 and 3 will be given here. Figures 13-22 show an arbitrary z-plane slice, near the center of the interaction region (z = 0.259 km) of species densities and reactions rates from the SOCRATES output for the ram case at 2.8 sec after the engine has been fired. The figures are plotted in the field of view of 20 by 20 km.

Figures 13-18 show the number densities of the atmospheric and engine species, as well as the species which are produced by the reactions shown in Table 3. In the figures, four features can be seen. First, the atmospheric species (O, O^+, and N_2) are depleted starting from the source (the shuttle's engine) and extending toward the wake of the shuttle for more than 5 km. For example, Figure 13 (a) shows the density distributions of atmospheric O atoms. It is evident that the O density has been depleted at the location of the shuttle engine and extends toward the wake of the shuttle. This depletion is produced by a combination of the chemical reactions in the ram and deflection of the O atoms. Second, the density of O atoms is increased in the ram direction due to the 'snow plow' effect. From Figure 13 (a), it can be seen that the density is enhanced about 15% above ambient values. Third, the exhaust species are concentrated mainly on the ram side of the shuttle. Fourth, N_2 is a common species between the atmosphere (9.2%) and exhaust (30.9%) compositions, and Figures 15 and 16 show that the N_2 is acting both like exhaust engine species, as well as an atmospheric species, as it shows some downstream depletion. In the same figures, the H_2O, which only exists in the exhaust composition, does not show any depletion. It should be noted that Figures 15 (a) and (b) are plotted based on the maximum and upper values of the densities and Figures 16 (a) and (b) are plotted based on a lower density range. As discussed earlier, the spatial distribution of the reaction rate for $O(^1D) \rightarrow O(^3P)$ emissions can be estimated by dividing the $O(^1D)$ density, given in Figure 13 (b), by the lifetime of 150 seconds.

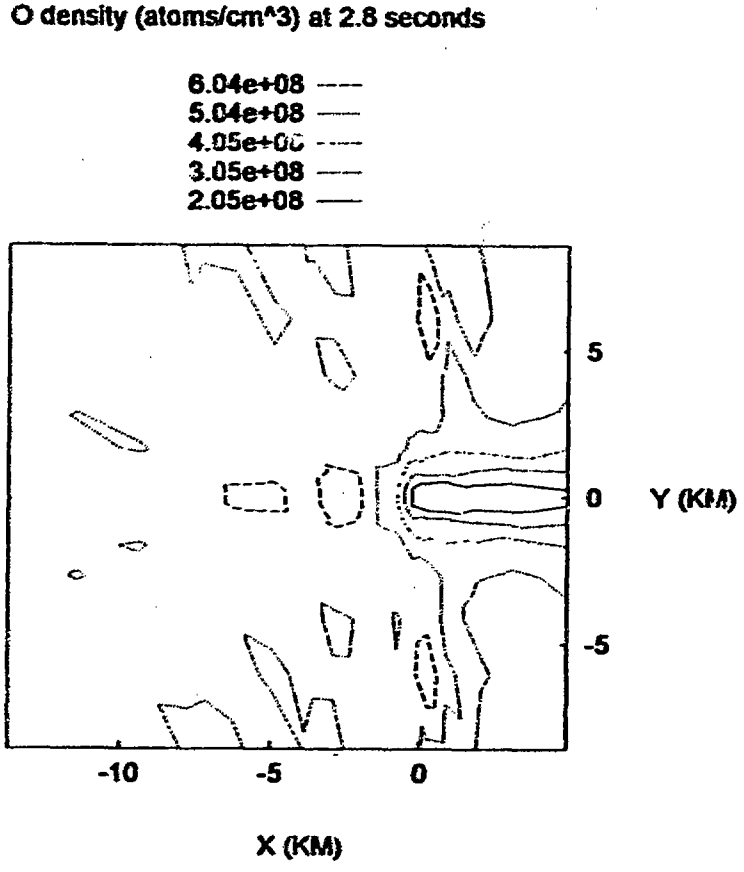

Figure 13(a). O densities on an arbitrary central z plane slice.

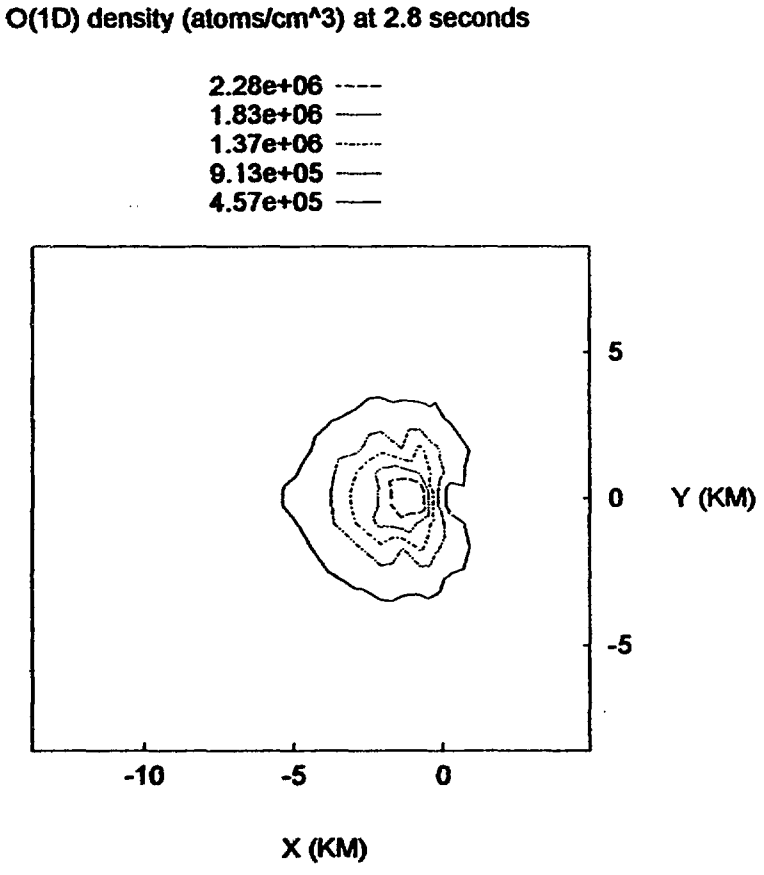

Figure 13(b). O(^{1}D) densities on an arbitrary central z plane slice.

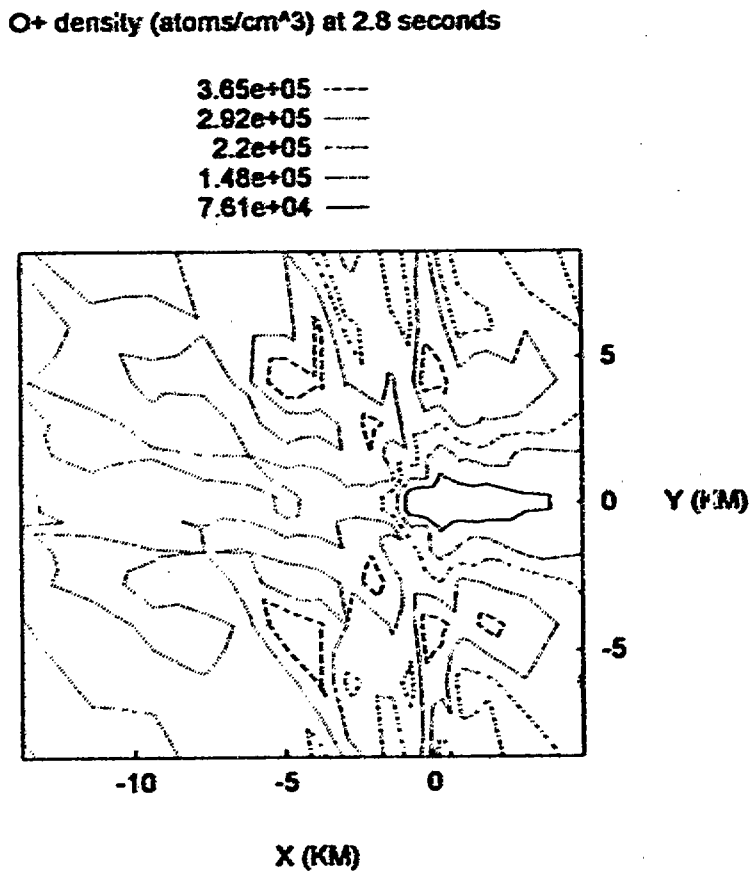

Figure 14(a). Charged O densities on an arbitrary central z plane slice.

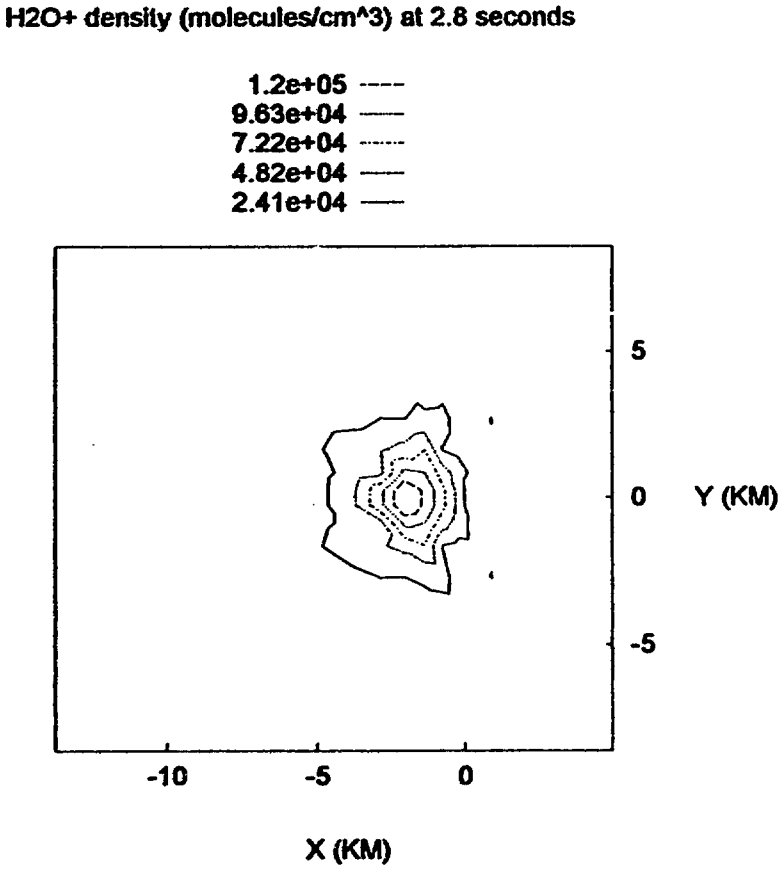

Figure 14(b). Charged H_2O densities on an arbitrary central z plane slice.

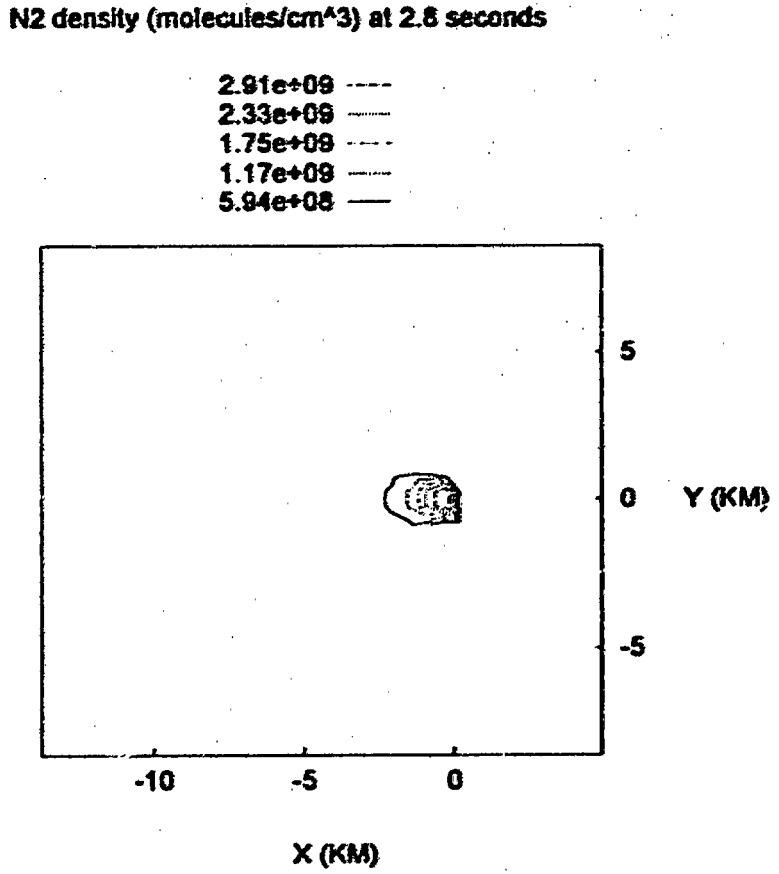

Figure 15(a). N_2 and densities on an arbitrary central z plane slice, plotted based on the maximum and upper values of the densities.

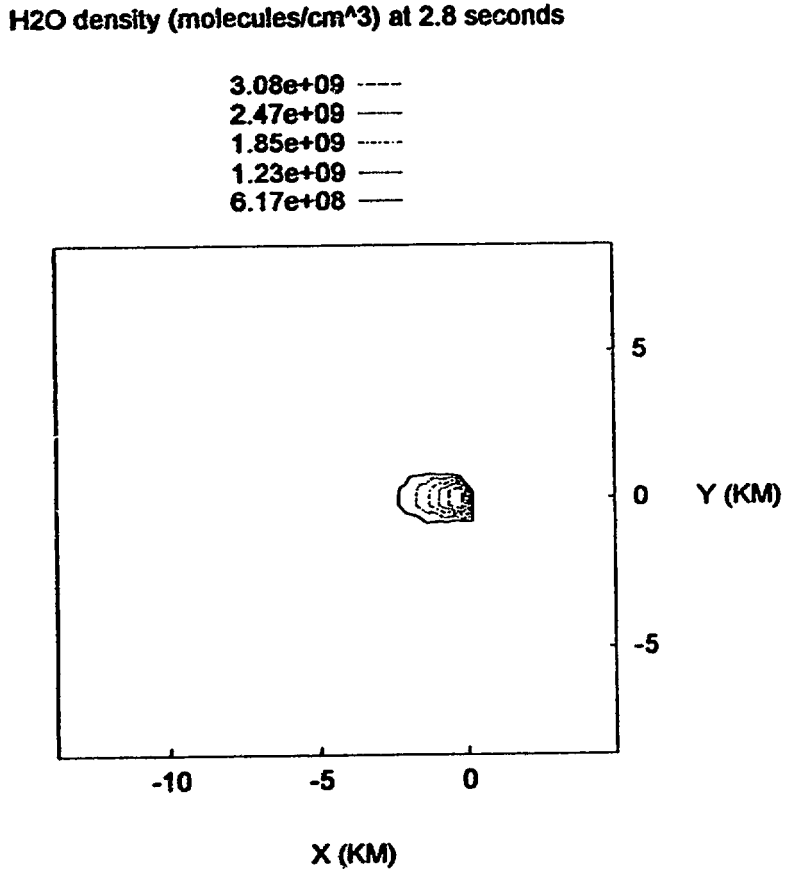

Figure 15(b). H_2O densities on an arbitrary central z plane slice, plotted based on the maximum and upper values of the densities.

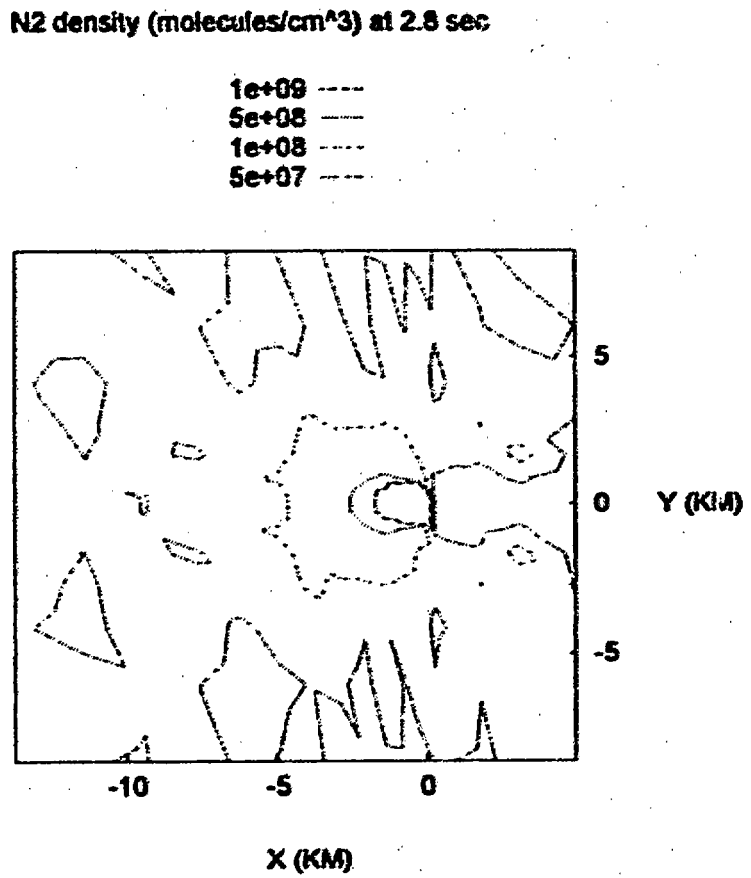

Figure 16(a). N_2 and densities on an arbitrary central z plane slice, plotted based on lower values of the densities.

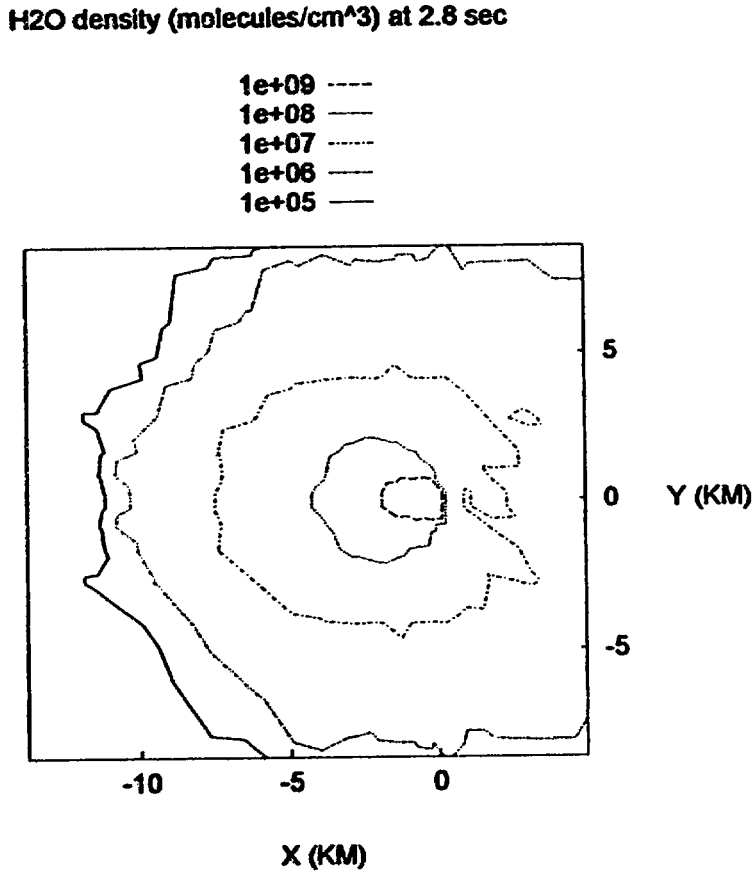

Figure 16(b). H_2O densities on an arbitrary central z plane slice, plotted based on lower values of the densities.

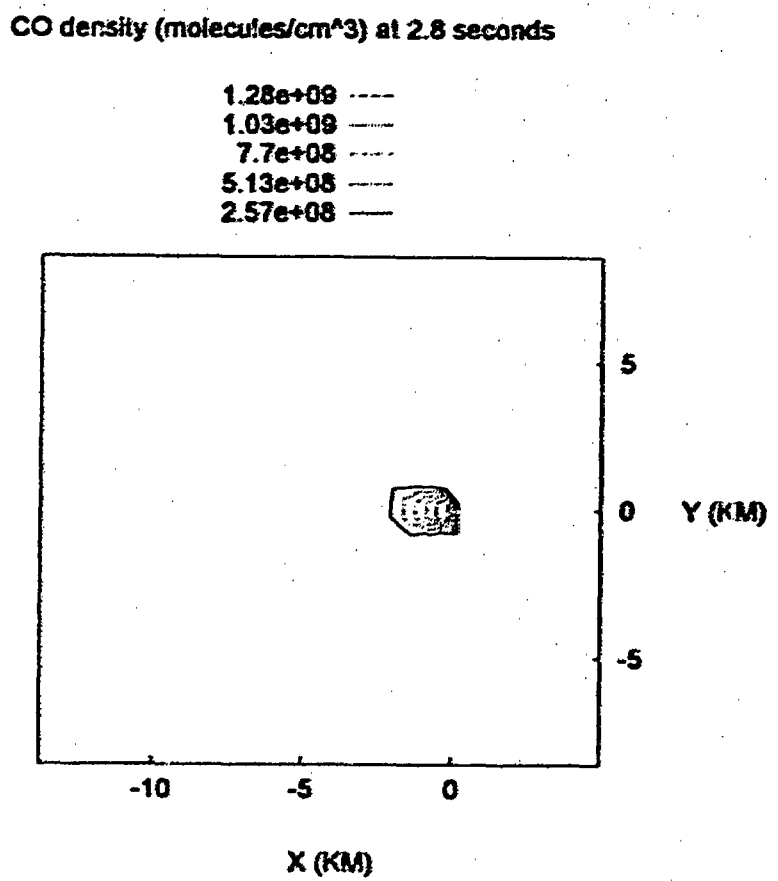

Figure 17(a). CO and densities on an arbitrary central z plane slice.

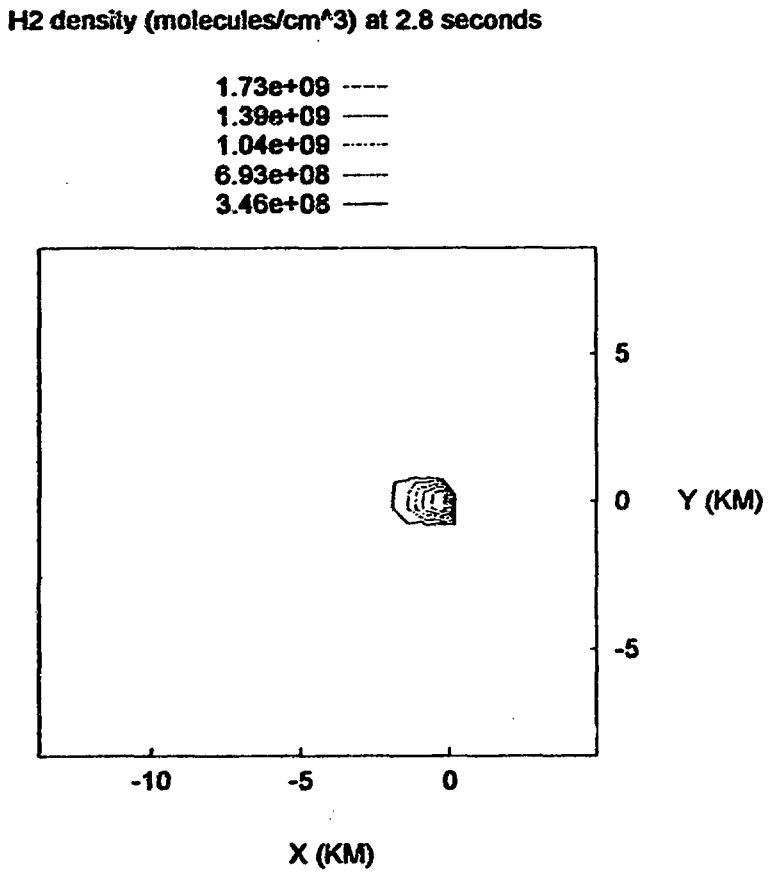

Figure 17(b). H_2 densities on an arbitrary central z plane slice.

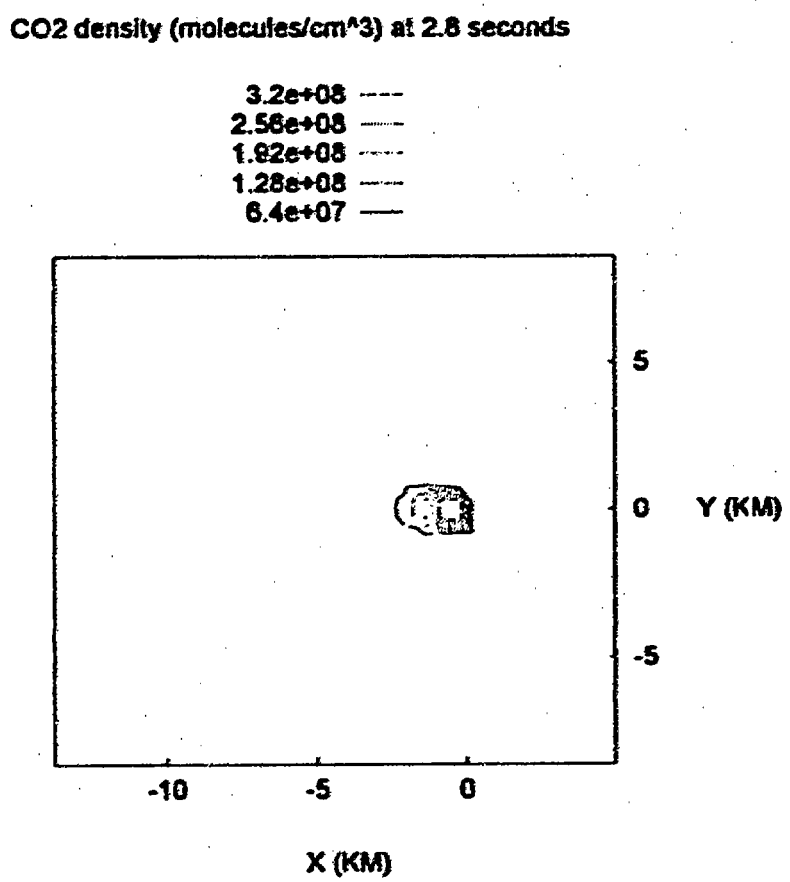

Figure 18(a). CO_2 and densities on an arbitrary central z plane slice.

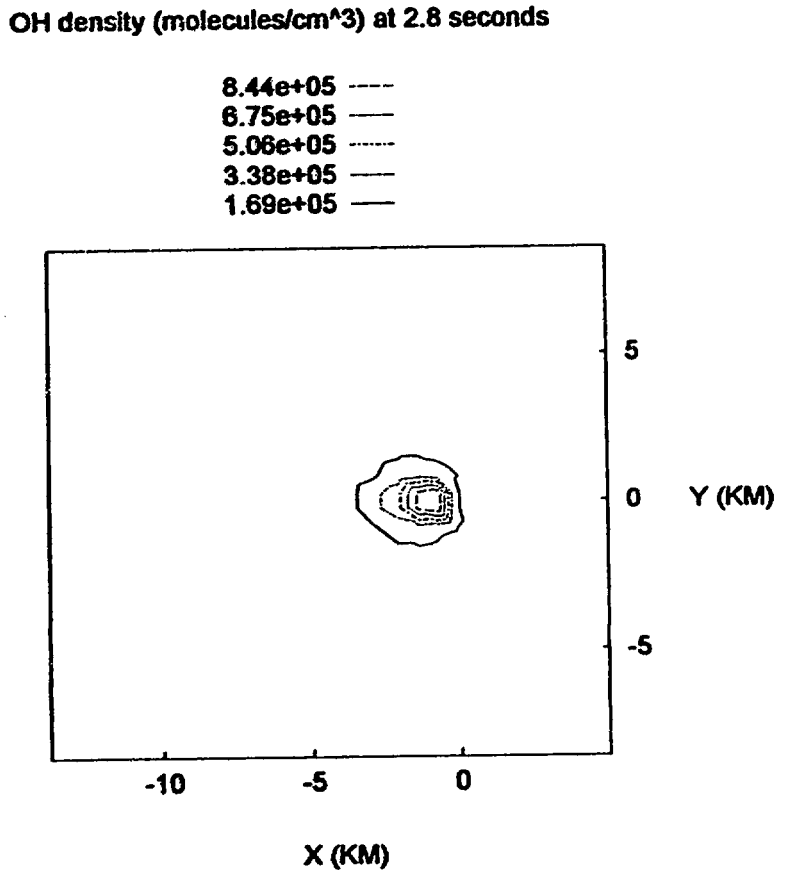

Figure 18(b). OH densities on an arbitrary central z plane slice.

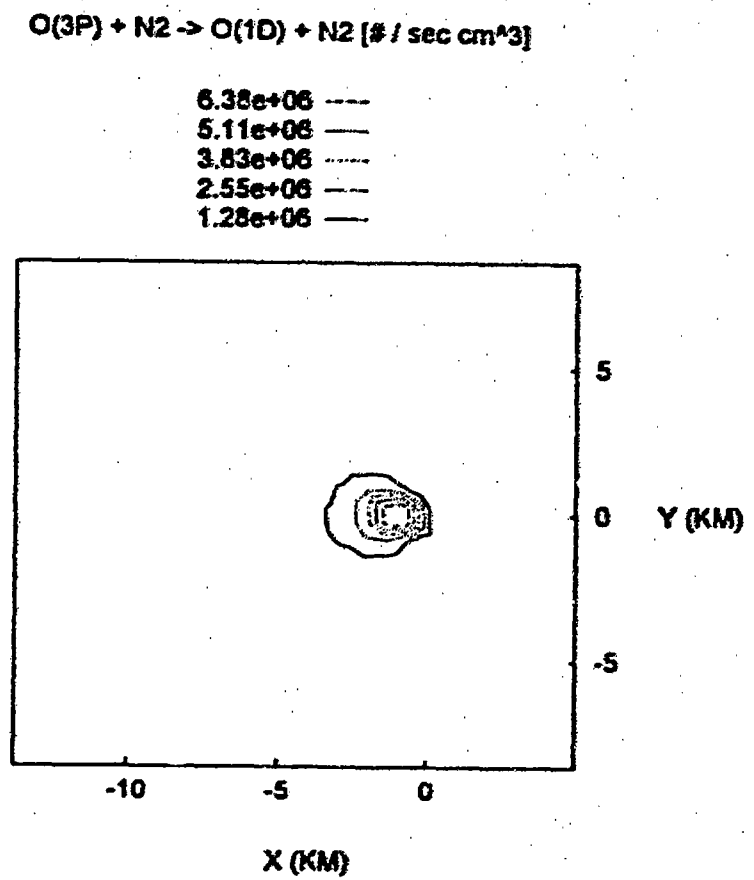

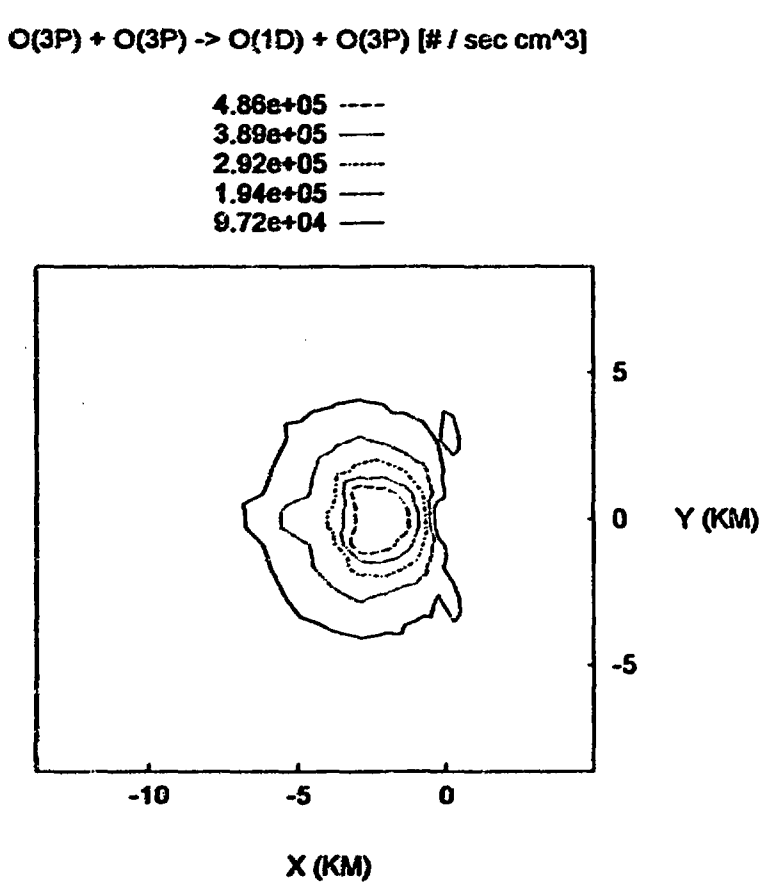

Figure 19. Reaction rates on an arbitrary central z plane slice, for reaction given above.

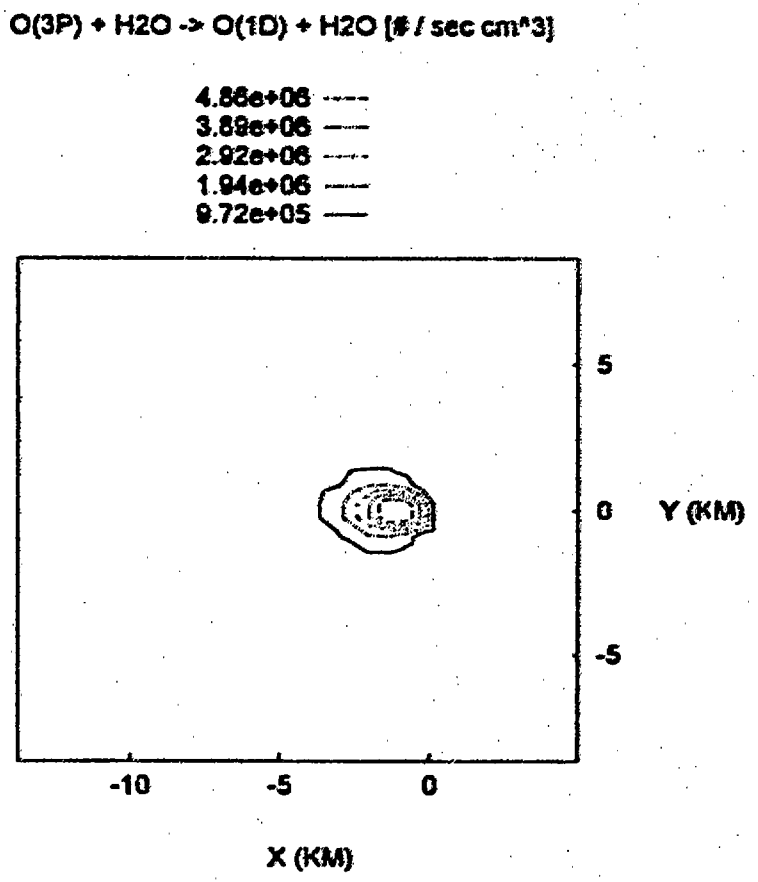

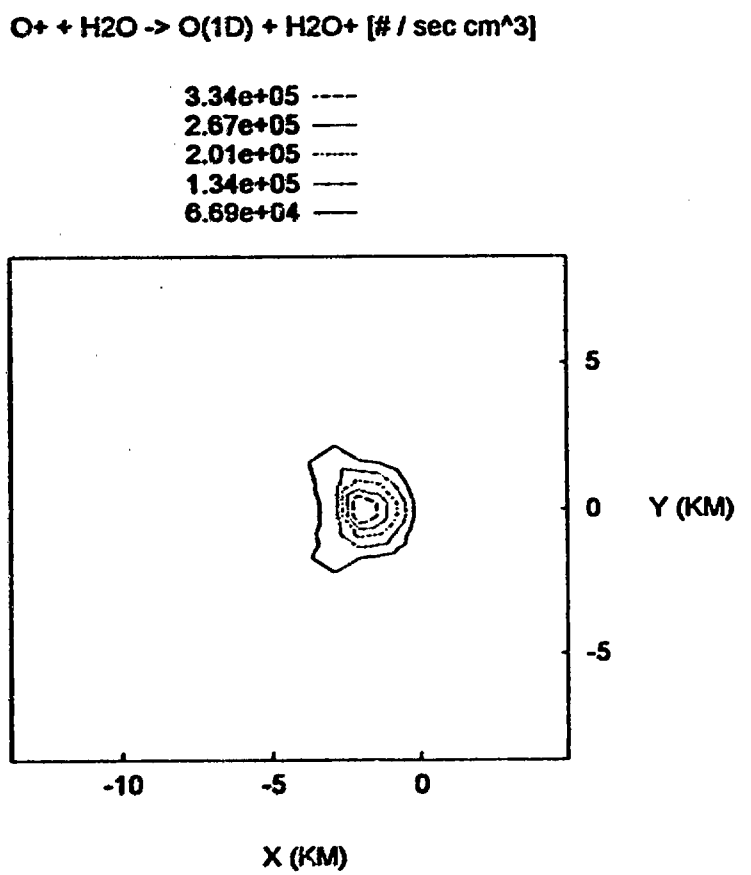

Figure 20. Reactions rates on an arbitrary central z plane slice, for reaction given above.

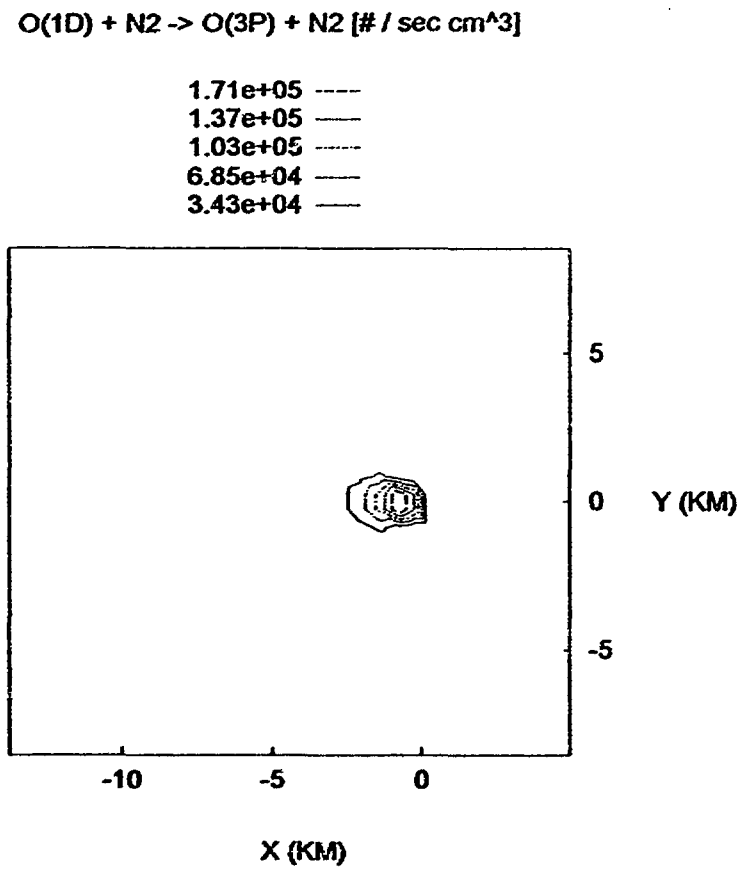

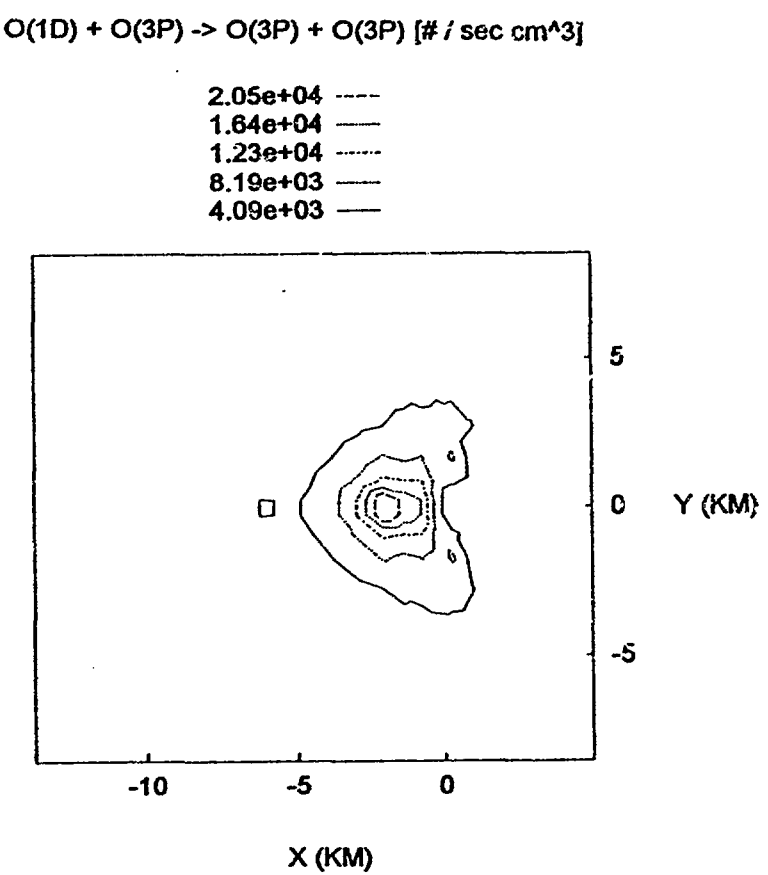

Figure 21. Reactions rates on an arbitrary central z plane slice, for reaction given above.

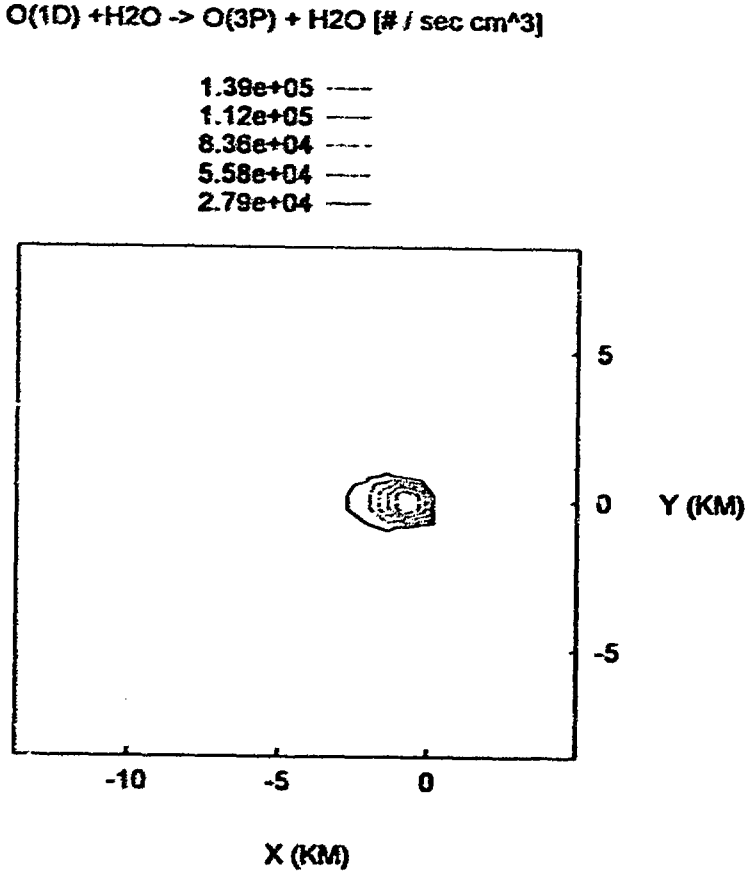

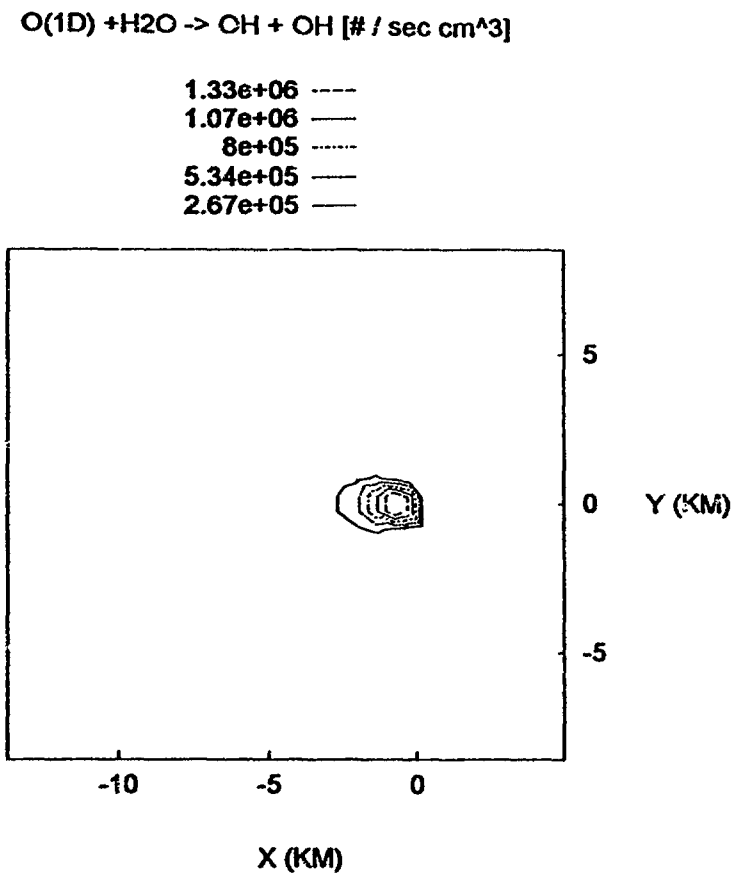

Figure 22. Reactions rates on an arbitrary central z plane slice, for reaction given above.

Figures 19-22 show the reaction rates (#/sec cm^3) for the reactions in Table 3. Figures 19 and 20 give the spatial distribution for the reactions that generate excited $O(^1D)$ atoms. The figures show that the dominant reaction rates occur in Figures 19 (a) and 20 (a), where an O atom collides with an N_2 molecule or a water molecule. Figures 21 and 22 represent the spatial distribution for the four quenching reactions given in Table 3. It can be seen that Figure 22 (b), where an O atom collides with a water molecule, shows the most intense quenching rate. The reaction rates generating $O(^1D)$ atoms are stronger than the quenching rates, so that the $O(^1D)$ density is increasing at time 2.8 seconds. The most intense generating reactions are concentrated near the shuttle and the excited $O(^1D)$ atoms diffuse out to form the plume.

5. SUMMARY AND CONCLUSION

The SOCRATES code was used to simulate the interactions between the PRCS engine firings and the ambient atmosphere in the three orientations of ram, perpendicular, and wake of the shuttle motion. The calculations were made at an altitude of 320 km. The simulation results indicated that when the exhaust of the space shuttle interacts with the ambient atmosphere, it generates long-lasting emissions at 6300 Å. The intensity of these emissions varied from strong to weak for ram to wake firings, respectively. The discussions of the intensity of $O(^1D \rightarrow {}^3P)$ transition photons as a function of firing directions (ram, perpendicular, and wake) and time were illustrated in Figures 1 through 6. A series of color plots was presented to show the plume developments as a function of time for the three orientations of engine firing (Figures 7 through 12). A series of figures was also shown to illustrate the involvement of other species and their reactions in the simulation (Figures 13-22).

REFERENCES

Bird, G. A., "Molecular Gas Dynamics", Clarendon Press, Oxford, 1976.

Bird, G. A., "Monte-Carlo Simulation in an Engineering Context", Proceeding of the 12th International Symposium on Rarefied Gas Dynamics, Prog. Astronaut. Aeronaut., Vol. 74, pages 239-255, 1981.

Borgnakke, C., and P. S. Larsen, "Statistical Collision Model for Monte Carlo Simulation of Polyatomic Gas Mixture", Journal of Computational Physics, Vol. 18, pages 405-420, 1975.

Broadfoot, A. L., E. Anderson, P. Sherard, D. Knecht, R. Viereck, C. P. Pike, E. Murad, J. B. Elgin, L. S. Bernstein, I. K. Kofsky, D. L. A. Rall, J. Blaha, and F. L. Culbertson "Spectrographic Observation at Wavelengths Near 630 nm of the Interaction Between the Atmosphere and the Space Shuttle Exhaust", Journal of Geophysical Research, Vol. 97, No. A12, Pages 19,501-19,508, December 1. 1992.

Elgin, J. B. and R. L. Sundberg, "Model Description for the SOCRATES Contamination Code", AFGL-TR-88-0303, Spectral Sciences, Inc., Burlington, MA, 01803, 1988, ADA205181.

Elgin, J. B., D. C. Cooke, M. F. Tautz, and E. Murad, "Modeling of Atmospherically Induced Gas Phase Optical Contamination From Orbiting Spacecraft", Journal of Geophysical Research, Vol. 95, No. A8, Pages 12197-12208, 1990.

Elgin, J. B., L. S. Bernstein, I. K. Kofsky, D. L. A. Rall, R. Viereck, D. Knecht, E. Murad, C. P. Pike, A. Setayesh, A. L. Broadfoot, "A Comparison of Shuttle Engine Firings in Space to Code Predictions", Proceedings of JANNAF Exhaust Plume Technology Meeting, U. S. Army Missile Command, Redstone Arsenal, AL, May 14-19, 1991.

Elgin, J. B. and L. S. Bernstein, "The Theory Behind the SOCRATES Code", PL-TR-92-2207, Spectral Sciences, Inc., Burlington, MA 01803, 1992, ADA259987.

Tautz, M. F., " IRMA: A Program for Three Dimensional Color Display of Data", PL-TR-93-2116, 1993.